Climate, soil, and vegetation controls on the temporal variability of vadose zone transport

C. J. Harman,[1] P. S. C. Rao,[2] N. B. Basu,[3] G. S. McGrath,[4] P. Kumar,[1] and M. Sivapalan[1,5,6]

Received 1 November 2010; revised 15 August 2011; accepted 20 August 2011; published 30 September 2011.

[1] Temporal patterns of solute transport and transformation through the vadose zone are driven by the stochastic variability of water fluxes. This is determined by the hydrologic filtering of precipitation variability into infiltration, storage, drainage, and evapotranspiration. In this work we develop a framework for examining the role of the hydrologic filtering and, in particular, the effect of evapotranspiration in determining the travel time and delivery of sorbing, reacting solutes transported through the vadose zone by stochastic rainfall events. We describe a 1-D vertical model in which solute pulses are tracked as point loads transported to depth by a series of discrete infiltration events. Numerical solutions of this model compare well to the Richards equation–based HYDRUS model for some typical cases. We then utilize existing theory of the stochastic dynamics of soil water to derive analytical and semianalytical expressions for the probability density functions (pdf's) of solute travel time and delivery. The moments of these pdf's directly relate the mean and variance of expected travel times to the water balance and show how evapotranspiration tends to reduce (and make more uncertain) the mass of a degrading solute delivered to the base of the vadose zone. The framework suggests a classification of different modes hydrologic filtering depending on hydroclimatic and landscape controls. Results suggest that variability in travel times decreases with soil depth in wet climates but increases with soil depth in dry climates. In dry climates, rare large storms can be an important mechanism for leaching to groundwater.

Citation: Harman, C. J., P. S. C. Rao, N. B. Basu, G. S. McGrath, P. Kumar, and M. Sivapalan (2011), Climate, soil, and vegetation controls on the temporal variability of vadose zone transport, *Water Resour. Res., 47*, W00J13, doi:10.1029/2010WR010194.

1. Introduction

[2] The complex, transient, nonlinear transport and transformation processes operating in the vadose zone determine the timing and magnitude of the delivery of surface-applied solutes to groundwater [*Raats*, 1981; *Rao et al.*, 1985a; *Wang et al.*, 2009]. Through these processes, the vadose zone acts as a hydrologic filter that transforms the variability of the climatic signals, coupled with a biogeochemical filter to retard and attenuate solute inputs [*Basu et al.*, 2011]. Understanding this filtering is important for assessing the risks associated with groundwater contamination of surface-applied solutes, such as pesticides [*Rao and Davidson*, 1980; *Rao et al.*, 1985b; *Gustafson*, 1989; *van Der Werf*, 1996; *Arias-este et al.*, 2008]. An important control on this temporal filtering is the reduction of soil water content by vegetation through root water uptake and the replenishing of this water content by the stochastic inputs of infiltration [*Struthers et al.*, 2006, 2007; *McGrath et al.*, 2007]. A full understanding of the temporal patterns of solute delivery through the vadose zone therefore depends not only on the processes of solute transport and degradation but also on the way these processes are controlled by the stochastic variability of the climate and the hydrologic filtering of this variability in the vadose zone.

[3] In previous work, several authors have examined solute transport through the root zone by assuming for simplicity that the flow is steady, thus neglecting the episodic (stochastic) transport processes [*Rao et al.*, 1985b]. In this work we examine the role of evapotranspiration in modifying the temporal variability of the transport of solutes carried through the vadose zone by the propagation of wetting fronts, using a low-dimensional model of this transport that lends itself ultimately to a semianalytical solution.

[4] Surface-applied solutes can migrate very rapidly to groundwater through preferential flow pathways, such as macropores, or more slowly through the bulk of the unsaturated zone [*Flury*, 1996]. While preferential flow can be important

[1]Department of Civil and Environmental Engineering, University of Illinois at Urbana-Champaign, Urbana, Illinois, USA.
[2]School of Civil Engineering and Department of Agronomy, Purdue University, West Lafayette, Indiana, USA.
[3]Department of Civil and Environmental Engineering, University of Iowa, Iowa City, Iowa, USA.
[4]School of Earth and Environment, University of Western Australia, Crawley, Western Australia, Australia.
[5]Department of Geography, University of Illinois at Urbana-Champaign, Urbana, Illinois, USA.
[6]Water Resources Section, Faculty of Civil Engineering and Geosciences, Delft University of Technology, Delft, Netherlands.

Copyright 2011 by the American Geophysical Union.
0043-1397/11/2010WR010194

for leaching, the vast majority of the chemical is transported through the slower flow pathways [*McGrath et al.*, 2007]. It is therefore important to understand the capacity of the latter domain to store and release these solutes. In this domain, the solutes are rarely flushed through the vadose zone in a single infiltration event. Rather, multiple events are required to carry a surface-applied solute through the vadose zone in a series of events, during which the solutes are mobilized by the flow [*Wang et al.*, 2009]. The depth to which water will infiltrate the soil and carry these solute loads through the profile is driven in part by the antecedent conditions of soil water content as well as by the rainfall characteristics and the hydraulic properties of the soil. Thus, the reduction of water content by root water uptake may serve to increase the residence time of solutes, particularly as they progress deeper through the profile and require larger events to mobilize them [*Destouni*, 1991]. The time delays associated with episodic and retarded transport through the vadose zone allow for various biogeochemical processes to transform and attenuate the solute pulses. For example, the degradation of pesticides in the vadose zone is vital to reducing groundwater contamination [*Flury*, 1996].

[5] The effects of transient infiltration on the travel time distribution of solutes through the vadose zone have been investigated extensively to determine whether this transport can be approximated by equivalent steady state flows [*Wierenga*, 1977]. *Russo et al.* [1989a, 1989b] suggested that solutes may travel faster through a soil profile under transient flow, while *Destouni* [1991] suggested that when the effects of root water uptake are accounted for, equivalent steady state flows could be used to predict the solute breakthrough curve. *Foussereau et al.* [2001] examined flow in a heterogeneous vadose-saturated zone system and found that while equivalent steady flow could predict the spatial structure of a solute plume, uncertainty in the timing of the solute delivery near the surface was dominated by the variability in the rainfall. More recently, *Russo and Fiori* [2008] found that at hillslope scales (where the water table was sufficiently deep) transport through soils could be conceptualized as occurring in two zones: a highly transient near-surface zone and a deep zone where flow was quasi-steady. *Fiori and Russo* [2008] found that the transient flows had little effect on the flow-corrected travel time distribution of a solute migrating through a heterogeneous hillslope. In other words, the transient flow determined the absolute travel time but did not create additional dispersion. Such equivalent steady state flows have been used to predict contaminant leaching risks [*Rao et al.*, 1985b]. In short, these studies suggest that the transience of flow created by the hydrologic variability of the vadose zone is an important determinant on the absolute travel time of a solute but has only a small effect, if any, on the dispersion of an individual solute pulse.

[6] However, the extent to which the stochastic variability in the rainfall amounts themselves influences the expected travel time of a solute and the exact nature of this influence are unclear. Moreover, in many cases they are applied to relatively humid systems, where the effects of evapotranspiration on the transport behavior may be small [*Destouni*, 1991]. Those who have used an analytical approach tend to neglect the effects of evapotranspiration. *Jury and Gruber* [1989] used the transfer function approach to examine the effect of climate variability on the travel time through the vadose zone. The transfer function predicts the solute delivery as a function of the total infiltration. Convolving this with the probability density function (pdf) of the total infiltration (conditional on time since solute application) gives the pdf of the travel time but neglects the effect of evapotranspiration noted above. A recent exception is given by *McGrath et al.* [2008a, 2008b, 2010a, 2010b], who used recent advances in stochastic modeling of the coupling of soil water and climate to directly examine the role of the hydrologic filtering on solute delivery to groundwater. They used a simple stochastic soil water model to assess the risk of pesticide leaching through preferential flow channels on the basis of the assumption that preferential flow was initiated when mean soil water content or rainfall intensity exceeded a threshold but did not examine the transport of the solute through the matrix itself.

[7] The stochastic soil water content models utilized by *McGrath et al.* [2008a, 2008b, 2010a, 2010b] provide an elegant framework for investigating how soil, climate, and vegetation properties control soil water variability and how this variability affects coupled processes. The approach was pioneered by *Eagleson* [1978] and *Milly* [1993] and was later expanded by *Rodriguez-Iturbe et al.* [1999] and others [see, e.g., *Laio et al.*, 2001; *Porporato et al.*, 2001]. In these works, precipitation is represented as a stochastic process (a marked Poisson process) with known properties. Simplified representations of soil water dynamics parametrized with measurable properties of the soil, climate, and vegetation (such as potential evapotranspiration, root zone depth, and soil hydraulic properties) can then be used to derive analytical expressions for key aspects of soil hydrologic variability. Expressions have been derived for the pdf of soil water content [*Laio et al.*, 2001], duration of plant water stress [*Porporato et al.*, 2001], mean frequency of recharge [*Botter et al.*, 2007], and other properties. The power of these approaches is in the way they reveal the dynamic variability of the vadose zone hydrology, the relative importance of different controls on that variability, and the relationship between the controls and other quantities of interest, such as the ecosystem functional behavior. Consequently, they can also provide a first-order estimate of the direction and magnitude of changes in system dynamics under changing climatic conditions [*Porporato et al.*, 2004].

[8] However, this stochastic soil water approach has not been applied to examine controls on the dynamics or functional behavior of reactive solute transport and transformations through the soil profile (as opposed to the preferential flow triggering examined by *McGrath et al.* [2008a, 2008b]). An impediment to using the stochastic approach for solute transport through the vadose zone is the need to resolve the travel time from the soil surface to the water table. Most applications of this type of stochastic soil water model have treated the root zone in a lumped way and have not considered the vertical variations in soil water content. *Guswa et al.* [2004] examined the validity of this assumption for ecohydrologic applications and found it to provide a reasonable approximation of the water balance dynamics. An exception is the work of *Laio et al.* [2006], who developed a vertically extended stochastic soil water content model and used it to predict optimal root distribution [*Laio*, 2006].

[9] *Rao et al.* [1985a] suggested a simplified framework for modeling solute transport through the vadose zone that is useful for investigating the role of hydrologic-biogeochemical

filtering. This framework is of a similar order of complexity as the stochastic soil water approach and relies on compatible assumptions of soil water content dynamics. In this approach, solute pulses are tracked as point loads undergoing retardation (linear, reversible, equilibrium sorption) and first-order degradation. The pulses are transported through the vadose zone in a series of discrete jumps associated with infiltration events, whose size depends on the amount of infiltration relative to the deficit of water storage created by evapotranspiration as well as the solute and soil properties.

[10] The discrete jumps in the *Rao et al.* [1985a] approach can be conceptualized as a stochastic process, similar to a random walk, whose jump sizes and the waiting time between jumps are driven by the stochastic rainfall process modified by the retardation and hydrologic filtering. This suggests that this approach to solute transport can be coupled to the stochastic soil water models to predict the delivery of reactive solutes through the vadose zone probabilistically in terms of the soil, climate, and vegetation properties.

[11] In this work we will use the approach of *Rao et al.* [1985a] and the stochastic soil water theory described above to investigate the temporal filtering of reactive solute delivery to the base of the vadose zone. Of particular interest is how the controls on this filtering affect the likely values (and variability) of the travel time through the vadose zone and the consequent degradation of solutes undergoing transformations with first-order kinetics. We will use a numerical implementation of the *Rao et al.* [1985a] approach, which allows results to be obtained for specific cases without further assumptions. We will also provide analytical and semianalytical solutions for the probability density functions, mean, and variance of quantities of interest, which provide deeper insight to the shifting importance of different controls across a range of conditions. These results can be seen as an extension of the work of *Jury and Gruber* [1989], except that here we neglect the effects of dispersion but account for the effects of evapotranspiration.

[12] The rest of the paper is structured as follows: in section 2 we describe the model, providing examples of typical numerical results and a validation against HYDRUS [*Šimůnek et al.*, 2009], a full Richards equation–based solution. In section 3 we develop a semianalytical solution to the stochastic model dynamics and test it against the numerical solutions. Then in section 4 we discuss the results, focusing on what is revealed about the role of hydrologic filtering on the timing and delivery of solutes through the vadose zone and the role of climate, soils, and vegetation in controlling this filtering.

2. Event-Based Model of Solute Transport in the Root Zone

[13] The vadose zone model developed here is a low-dimensional model that combines a soil water framework amenable to the stochastic models developed by *Milly* [1993] and *Rodriguez-Iturbe et al.* [1999] with the solute transport model of *Rao et al.* [1985a]. For convenience we will refer to this model as HEIST (HEIST event-based infiltration and solute transport model). The model is intended to provide insights into the dynamics of the upper part of the vadose zone, where root water uptake is a significant part of the water balance. For simplicity, we assume a homogeneous profile of soil and root properties. The soil water content varies throughout the profile and through time as a result of the inputs from infiltration and losses from drainage and evapotranspiration. We adopt constant values of the sorption and degradation solute properties (defined in section 2.2), which must be regarded as effective properties.

2.1. Soil Water Storage Dynamics

[14] Soil water mass balance in a uniform soil at a depth z is typically expressed as [*Laio*, 2006]

$$\frac{\partial \theta(z,t)}{\partial t} = -\frac{\partial q(z,t)}{\partial z} - U(z,t), \tag{1}$$

where $\theta(z, t)$ is the volumetric soil water content, $q(z, t)$ is the soil water flux, and $U(z, t)$ is the rate of uptake of water by plants. At the upper boundary of the soil ($z = 0$) the flux $q(z, t)$ into the soil is the infiltration rate $I(t)$, which is the rainfall rate reduced by losses to interception and surface runoff. Typically, the solution of this equation under variable $I(t)$ requires numerical modeling because of the nonlinear dependence of $q(z, t)$ on the soil water content and hydraulic potential gradients in the soil and the dependence of $U(z, t)$ on atmospheric water demand and the regulation of stomatal conductance by vegetation.

[15] Here we will adopt a significantly simpler approach that is similar to other vertically extended stochastic soil water models that have been used for similar purposes recently, such as by *Schenk* [2008], *Guswa et al.* [2004], and *Laio et al.* [2006]. This approach is motivated by the observation that the infiltration and redistribution of rainfall in well-drained soils operate on a much shorter time scale than the time between storm events. We can therefore treat the infiltration and subsequent redistribution of water in the soil profile as an event that occurs effectively instantaneously. The infiltrated water forms a sharp "wetting front," below which water content is unaffected by the advancing front (this model is therefore most appropriate in soils that drain quickly, such as those with low clay content). This approach is similar to that assumed by the Green and Ampt infiltration model [*Green and Ampt*, 1911] and the multiple wetting front model of *Struthers et al.* [2006] and was investigated by *Milly* [1985], who found that it was appropriate in soils where the second derivative of the hydraulic conductivity with respect to soil moisture is strictly positive, a condition that is usually satisfied. The position of the wetting front after redistribution is determined by assuming that it effectively ceases to advance once the water content of the soil profile above it reaches some threshold value θ_{fc}. This value represents the water content at which the hydraulic conductivity of the redistributing front becomes in some sense "small" compared to the process of evapotranspiration. The ability of the model to reproduce the water balance and solute dynamics has been validated against the full solution of the Richards equation (see auxiliary material).[1] This model is given in precise terms below and is illustrated in Figure 1. Given an initial water content profile $\theta(z, t_i^-)$ (where t_i^- indicates the time just prior to the storm at time t_i), the effect of the infiltration and redistribution of the

[1] Auxiliary materials are available in the HTML. doi:10.1029/2010WR010194.

volume of water $I(t_j)$ is to raise the water content of the surface soils to θ_{fc} down to a depth z_i given by

$$I(t_i) = \int_0^{z_i} \left[\theta_{fc} - \theta(z, t_i^-)\right] \mathrm{d}z. \quad (2)$$

[16] In other words, the infiltrated water fills the deficit between θ_{fc} and the initial water profile $\theta(z, t_i^-)$. Note that (as shown in Figure 1) the water at the lower edge of the wetting front will be composed of "old water" that has been displaced down the profile. Drainage through a reference plane at the base of the root zone Z_r occurs when the sum of the initial soil water content and the infiltrating water is greater than the total storage above the reference plane at field capacity $Z_r\theta_{fc}$.

[17] The infiltration amount $I(t_i)$ must be related to the rainfall depth $P(t_i)$ by considering the precipitation intensity and the constraints imposed by the infiltration capacity of the soil. We can incorporate this effect while retaining the instantaneous description of the process by using a model of the infiltration capacity as a function of total infiltration. Here we use the Green and Ampt model, modified to account for the profile of water content. This model, like the framework described above, assumes a sharp wetting front of infiltration, driven by gravity. The infiltration rate over the course of a storm is given by a linear approximation of the water potential gradient between the soil just below the wetting front and the ponded surface. The modification simply involves allowing the water potential below the wetting front to vary over the course of the infiltration event in line with the actual profile of water content $\theta(z, t_i^-)$, rather than having a fixed value.

[18] Between storm events i and $i + 1$, evapotranspiration removes an amount of water $E(t_i)$ from the profile (Figure 1). We will neglect soil evaporation and consider only the effect of root water uptake on $E(t_i)$. Root density distributions for annual crops (to which pesticides are commonly applied) are more likely to decline exponentially with depth and to grow deeper with time over the growing season [*Bengough et al.*, 2006]. Here we neglect such effects. For the purposes of examining the role of evapotranspiration on solute transport, we will define the reference plane Z_r as the base of the root zone and assume that the root properties are uniform over the profile. The model of evapotranspiration must determine both the quantity of water to be removed from the root zone between one storm event and the next and from where in the profile the water is removed. Many models of different complexity exist in the literature. We adopt two alternative approaches here so that the results will be comparable to two other soil water models. The first is the simpler approach used in the stochastic soil water models [*Porporato et al.*, 2004], which determines the uptake rate as limited by a maximum rate $\mathrm{ET}_{\max}$ and reduced below this maximum by a function of the average water content of the profile. The instantaneous rate of evapotranspiration is therefore

$$e(t) = \mathrm{ET}_{\max} f[\bar{\theta}(t)], \quad (3)$$

where $\bar{\theta}(t)$ is the vertically averaged water content in the soil and $f[\bar{\theta}(t)]$ is linear between θ_{pwp} and θ_{fc}:

$$f[\bar{\theta}(t)] = \frac{\bar{\theta}(t) - \theta_{pwp}}{\theta_{fc} - \theta_{pwp}}. \quad (4)$$

[19] The total water extraction between time steps t_i and t_{i+1} can then be given by integrating this equation analytically from one time step to the next:

$$E(t_i) = \mathrm{ET}_{\max} \int_{t_i}^{t_{i+1}} f[\bar{\theta}(t)]\mathrm{d}t, \quad (5)$$

$$= Z_r\left[\bar{\theta}(t_i) - \theta_{pwp}\right]\left[1 - \exp\left(-\frac{\mathrm{ET}_{\max} t}{Z_r(\theta_{fc} - \theta_{pwp})}\right)\right]. \quad (6)$$

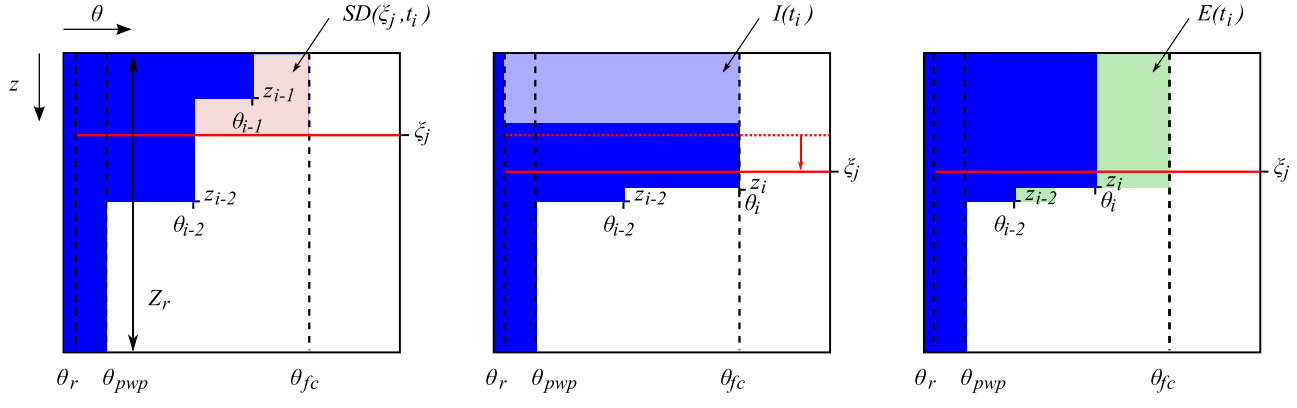

Figure 1. Representation of water and solute dynamics in the HEIST model. The infiltration $I(t_i)$ from rainfall event i forms a sharp wetting front that displaces antecedent moisture in the profile. After redistribution the upper part of the profile has a maximum water content at field capacity θ_{fc}, and the lower part is unchanged. The transport of the solute load centered at depth ξ_j depends on the difference between the infiltration $I(t_i)$ and the storage deficit in the soil above it $\mathrm{SD}(\xi_j, t_i^-)$, as well as the fraction of the pore volume participating in transport $(\theta_{fc} - \theta_r)$. Evapotranspiration $E(t_i)$ is removed from the profile between one storm and the next, creating this storage deficit (which has a lower bound at θ_{pwp}).

[20] Once calculated, the depth of water $E(t_i)$ is removed from the profile by removing it first from the wetting front with the highest water content (which is always at the surface) until the water content equals that of the next wettest front; extraction then continues from both these fronts and sequentially deeper ones until $E(t_i)$ is met. Note that this scheme results in a nonuniform distribution of root water uptake that preferentially removes water from the wetter upper parts of the soil, although we have not specified a nonuniform root depth distribution.

[21] The second model follows the *Feddes et al.* [1978] model used in HYDRUS [*Šimůnek et al.*, 2009], which will be used to validate the solute transport model. This model also assumes as an input a maximum rate of evapotranspiration $\mathrm{ET}_{\max}$. We chose to use the simplest version of the model, without uptake compensation. In this model, root water uptake is determined from each wetting front w in the profile as a function of water potential $\psi_w(t)$, rather than water content:

$$f[\psi_w(t)] = \frac{\psi_w(t) - \psi_{pwp}}{\psi_{fc} - \psi_{pwp}}, \tag{7}$$

where $\psi_w(t)$ is determined from the water content in each wetting front using an appropriate water retention function, such as the Brooks-Corey formulation. The instantaneous rate of extraction of water from each wetting front is then determined by the maximum rate $\mathrm{ET}_{\max}$ and the proportion of the total soil depth taken up by that wetting front. The total ET is then the sum of these:

$$e(t) = \mathrm{ET}_{\max} \sum_{w \in W} f[\psi_w(t)] \frac{\Delta_w}{Z_r}, \tag{8}$$

where Δ_w is the thickness of the soil between two wetting fronts. The total extraction is calculated by numerical integration between time steps. Note that we neglect the role of root stress under very wet conditions that appears in the *Feddes et al.* [1978] model, as we are primarily concerned with well-drained soils.

[22] Note that in both these models the soil water content is always below θ_{fc}, and so actual evapotranspiration rate is always less than $\mathrm{ET}_{\max}$. If water content were able to exceed field capacity, then the behavior of these two models would be qualitatively different. When the water content is calculated in the first model, wet surface layers and dry lower layers are averaged together. In the second model, where uptake rates are calculated for each wetting front individually, the uptake rate in the wet layers would be capped at the maximum and could not balance the lower values in dryer layers. In the formulation used here, however, the difference is minimal.

2.2. Solute Transport and Degradation

[23] Solutes are assumed to be transported through the soil by the advective flux of water, neglecting diffusion and dispersion. Observed solute spreading arises from processes at three scales: (1) molecular diffusion at scales of a few centimeters due to concentration gradients, (2) hydrodynamic dispersion at scales of <1 m due to variations in local flow velocity, and (3) macrodispersion at the scale of several meters due to spatial heterogeneity in hydraulic properties and flow pathways. Here we will neglect all these forms of spreading in order to focus on the range of travel times created by the effects of variable climate inputs on infiltrating water. Thus the results could be regarded as a good approximation of a plume traveling through the vadose zone that is not significantly dispersed by the time it reaches the depth of interest. Where dispersion is larger, the method will provide systematic underestimates of travel times. However, as *Rao et al.* [1985a] suggest, if the point loads simulated here are representative of the position of the centroid (or perhaps more accurately the leading edge) of a plume, the approach could be adapted in future work to simulate the position of the centroid of an advecting plume even where dispersion is not negligible. This approach is further justified by the observations cited in the introduction that the transient water dynamics have little effect on the shape of the solute plume and primarily affect the timing of the solute delivery, which is captured here by the arrival of the point load at the base of the root zone [*Destouni*, 1991; *Foussereau et al.*, 2001; *Russo and Fiori*, 2008; *Fiori and Russo*, 2008]. It should again be noted that we are explicitly excluding soils in which macropore flow is significant.

[24] Under these assumptions, *Rao et al.* [1985a] suggested the following piston model of the transport of reactive solute point loads through the vadose zone. Let us assume that a storm event at time t_i carries into the soil a mass of solute M_i. This mass may be carried by the rainfall (e.g., wet deposition) or released and leached into the soil from some surface source zone (e.g., applied fertilizers, nutrients, and pesticides). The point load mass is carried into the soil by the infiltrating water, and its final position after redistribution ξ_i is proportional to the depth of wetting front penetration $I(t_i)/(\theta_{fc} - \theta_r)$ and inversely proportional to a retardation factor R that accounts for the effects of linear, equilibrium, and reversible sorption-desorption processes:

$$\xi_i(t_i) = \frac{I(t_i)}{R(\theta_{fc} - \theta_r)}. \tag{9}$$

[25] The residual water content θ_r represents the fraction of the pore water volume that is not displaced by the infiltrating water. Solute may undergo diffusional exchange with this volume and thus represent an "immobile" zone; however, this exchange is not represented here. The retardation factor for pesticides is a function of the soil bulk density ρ_b, organic matter fraction f_{OC}, equilibrium sorption coefficient (normalized to organic carbon) K_{OC}, and soil water content θ:

$$R = 1 + \frac{\rho_b f_{\mathrm{OC}} K_{\mathrm{OC}}}{\theta}. \tag{10}$$

[26] R varies from 1 to ∞, representing no retardation ($K_{\mathrm{OC}} = 0$) to complete sorption ($K_{\mathrm{OC}} = \infty$), respectively [*Rao et al.*, 1985a]. Here we are assuming that soil organic matter is the primary sorption domain, but this definition can easily be altered to allow for sorption to other soil components and to explicitly consider nonlinear sorption isotherm models. The retardation factor, as defined here, is a function of soil water content. We will make the assumption that an effective retardation factor can be obtained that

represents the retardation that occurs during transport. This assumption is tested in the auxiliary material.

[27] After being transported into the soil, solute point loads are transported deeper into the soil by a series of wetting fronts that propagate from rainfall events. The volume of water that transports a point load is reduced because of the storage deficit created by evapotranspiration above the point load. The storage deficit (SD) above a point load at depth ξ_j at time t_i is defined as (see Figure 1)

$$\mathrm{SD}(\xi_j, t_i^-) = \int_0^{\xi_j} \left[\theta_{fc} - \theta(z, t_i^-)\right] \mathrm{d}z. \tag{11}$$

[28] Therefore, the infiltration at time t_i, $I(t_i)$, will advect a point load initially at point $\xi_j(t_i^-)$ to a depth given by

$$\xi_j(t_i^+) = \xi_j(t_i^-) + \begin{cases} \dfrac{I(t_i) - \mathrm{SD}\left[\xi_j(t_i^-), t_i^-\right]}{R(\theta_{fc} - \theta_r)} & I(t_i) > \mathrm{SD}\left[\xi_j(t_i^-), t_i^-\right] \\ 0 & \text{otherwise} \end{cases}. \tag{12}$$

[29] Thus, each rainfall pulse infiltrating into the soil profile has to be larger than the soil water deficit above the current solute pulse location before further solute displacement occurs. As a consequence, the effective events that cause solute transport at depth in the profile are a filtered form of the rainfall events arriving at the surface.

[30] The point loads are lost from the root zone when they cross the reference plane Z_r. The age of the point load when it is lost from the system is given by $T_i = t_e - t_i$, the difference in the time of the infiltration event that carried it into the soil t_i and t_e, the time of the event that carried it past the reference plane Z_r. Note that if a point load is carried completely through the system in one event, $T_i = 0$. When the retardation and degradation are absent ($R = 1$ and $k_d = 0$), the solute load represents a nonreactive tracer, and its age T_i can be regarded as being representative of the age of the water carrying it through the system, allowing the water leaving the system to be "dated."

[31] Many solutes undergo complex biotic and abiotic transformations that alter their mass in the soil because of intracellular and extracellular microbial transformations, inorganic reactions with the soil constituents, and uptake by plants [*Flury*, 1996; *Jury et al.*, 1982; *Rao et al.*, 1985a]. Here we assume a simple first-order transformation model, with a rate constant k_d to approximate the solute loss during transport through the soil profile. Degradation and sorption characteristics can vary significantly over the soil profile (particularly for aerobic processes) [*Issa and Wood*, 1999]. We assume here that an effective rate constant to represent approximate first-order losses in the vadose zone can be estimated and used in the model. The mass remaining after a point load (with initial mass M_i) has traversed the vadose zone is then given by

$$M_e = M_i \exp(-k_d T_i). \tag{13}$$

[32] Where there are multiple transformation pathways, k_d represents the pooled loss through all loss pathways. If all loss processes are first-order, we can treat k_d as the sum of their individual contributions. We can define the delivery ratio (DR) as the ratio of the point load of solute mass of solute that enters the soil at t_i and the mass that is advected past the reference depth Z_r at t_e:

$$\mathrm{DR} = \frac{M_e}{M_i} = \exp(-k_d T_i). \tag{14}$$

[33] This is also known as the "attenuation factor" [*Rao et al.*, 1985b]. In principle, it is possible to extend the present analysis by invoking more complex models and by considering the fate of various by-products of degradation. However, our initial goal here is to consider the interaction between retardation, degradation, and episodic transport to illustrate the hydrologic and biogeochemical filtering of the root zone.

2.3. Typical Results for Various Solutes, Soils, Climates, and Validation

[34] Example results illustrating this model were obtained using a similar set of parameters as that used by *Jury and Gruber* [1989]. The results were compared to comparable runs of HYDRUS 1-D [*Šimůnek et al.*, 2009]. This validation showed that the water balance and solute transport predictions of this simplified model are very similar to that of HYDRUS 1-D. This validation is presented in the auxiliary material accompanying this paper.

[35] In these example runs, the root zone was assumed to be homogeneous. Soil parameters are given in Table 1 for a coarse soil with low organic carbon content, such as a sandy loam soil, and a finer soil with larger organic carbon content and a deeper biologically active zone. Note that the coarse soil has a very low plant available water (5.4%). Following the stochastic approach of *Rodriguez-Iturbe et al.* [1999], we assume that rainfall can be represented by a marked Poisson process with arrival rate λ_p and an exponential distribution of event sizes with mean depth α. These parameters and $\mathrm{ET}_{\max}$ were fixed constants for these simulations. Climate properties are given in Table 2 for (1) a humid climate, with low potential evapotranspiration and small frequent storms, representative of the marine climates of the Atlantic coast of the United States, and (2) a semiarid climate, with large, infrequent storms, such as what might be found in the southwestern United States.

[36] The migration through the root zone of four pesticides, applied to these hypothetical soils once a year, was

Table 1. Soil Properties Used for the Example Simulations and for Validation of the Model Against HYDRUS[a]

Parameter	Symbol	Coarse	Fine	Unit
Bulk density	ρ_b	1.5	1.2	g cm^{-3}
Organic carbon	F_C	0.2	1	% weight/weight
Depth	Z_r	500	1000	mm
Field capacity	θ_{fc}	10	20	% vol/vol
Wilting point	θ_{pwp}	4.6	6.0	% vol/vol
Plant available water	θ_{paw}	5.4	14	% vol/vol
Saturated water content	θ_{sat}	0.40	0.45	% vol/vol
Air entry pressure	Ψ_a	478	121	mm
Saturated hydraulic conductivity	K_{sat}	15.2	0.601	m d^{-1}
Brooks-Corey exponent	n	37.5	28.2	% vol/vol

[a]Note that plant available water θ_{paw} is simply the difference between field capacity and wilting point.

Table 2. Climate Properties for the Example Simulations

Parameter	Symbol	Humid	Semiarid	Unit
Storm frequency	λ_p	0.3	0.047	1 d^{-1}
Storm depth	α	8.5	23	mm
Maximum evapotranspiration	ET_{max}	600	1000	mm yr^{-1}
Dryness index	ϕ	0.64	2.5	

examined. To focus on the transformations within the root zone, the dynamics of pesticide degradation following application and prior to the first storm were neglected. A unit mass of each pesticide was assumed to enter the soil in the first storm following application. These pesticides have a variety of properties and were selected because of their widespread use and potential to contaminate the environment (see Table 3). Pesticide profiles are available from EXTOXNET (http://pmep.cce.cornell.edu/profiles/extoxnet/) and are also available from *Hornsby et al.* [1996]. Atrazine is a widely used herbicide in the United States but is banned in the European Union. It has moderate sorption properties and an intermediate decay rate. Atrazine (A) is moderately toxic to humans and has been classified as possibly carcinogenic by the U.S. Environmental Protection Agency. Bromacil (B) is also a herbicide and is similarly moderately toxic and possibly carcinogenic. However, it is more weakly sorbing than atrazine and has a longer half-life in the environment. Ethylene dibromide (ED) is a fungicide and a fuel additive. It is highly toxic, carcinogenic, weakly sorbing, volatile, and resistant to degradation. (Note that we do not account for vapor losses in the current model, which are likely to be particularly significant for ethylene dibromide.) Oxamyl (Ox), an insecticide, is extremely toxic and very weakly sorbing but degrades quickly.

[37] Figure 2 illustrates how soil and climate properties affect pesticide transport through the root zone. All of the pesticides leach quickly through the coarse soil in both climates, though only bromacil and ethylene dibromide (which have half-lives >300 days) reach the reference depth Z_r without significant degradation. The higher retardation and faster degradation of atrazine (half-life $= \log(2)/k_d \sim 64$ days) reduce its delivery in the humid climate and greatly reduce its delivery in the dry climate. Oxamyl degrades so quickly (half-life of ~6 days) that it only reaches the base if a sufficiently large storm (or series of storms) occurs soon after application. This can occur under both climates because the semiarid climate has large average storms and the humid climate has a high average initial water content so the storms driving the transport need not be so large.

[38] The results from the finer soil reveal a striking ability of evapotranspiration to delay transport compared to the coarse soil and a stronger contrast between the climates for the more persistent pesticides. Atrazine and oxamyl both degrade near the surface of the soil profile in both climates.

Table 3. Pesticide Properties for the Example Simulations

Parameter	Symbol	Atrazine	Bromacil	Ethylene Dibromide	Oxamyl	Unit
OC sorption	K_{OC}	160	72	44	6	$cm^3\ g^{-1}$
Degradation rate	$1/k_d$	92	505	5266	9	days

In a humid climate, bromacil reaches the base of the vadose zone after about 200 days of transport with some moderate degradation, and ethylene dibromide arrives in slightly less time with almost none. In the semiarid climate, however, the low transport rates in the lower vadose zone delay the transport further, leading to a long residence time and the potential for accumulation in the soil profile. Thus, the strongest potential for contamination is for the chemicals bromacil and ED and in coarse soil. However, even for these pesticides, retention within the root zone for fine soils and semiarid climate may be long enough to significantly reduce leaching risks.

3. Solute Leaching as a Stochastic Process

[39] The filtering of the solutes through the vadose zone illustrated in Figure 2 is determined by the combination of soil, climate, and solute properties and, in particular, from the spatial and temporal hydrologic variability of the vadose zone. Our simulations suggest that the roles played by climate and soil properties have a complex set of interactions. Motivated by the desire to get a broader view of this interaction, we will seek expressions for the pdf of the residence time and delivery ratio of such surface-applied sorbing, degrading solutes to these properties that explicitly incorporate climatic and soil properties. We start by examining the distribution of transport event sizes and waiting times using the numerical model. Using the results, we will then lay out a general framework for the derivation under some simple assumptions and then derive the results under the special case that there is no evapotranspiration. The expressions obtained are similar to those of *Jury and Gruber* [1989]. We then utilize the results of a Monte Carlo simulation with the HEIST model to obtain a semianalytical expression for the pdf of travel times where evapotranspiration creates variations in the water content with depth. This semianalytical model will then be evaluated against the numerical HEIST approach developed in section 2.

3.1. Distribution of Transport Event Sizes and Waiting Times

[40] Here we will develop expressions for the distribution of jump sizes and waiting times of transport events through the vadose zone. To do so, we will make use of the class of stochastic soil water models derived from the work of *Rodriguez-Iturbe et al.* [1999]. This model uses a lumped conceptualization of soil water in which the vadose zone is treated as a single unit. Although the model described above resolves the vertical profile of soil water, drainage events are only triggered when an infiltrating event raises the average water content of the whole profile above the threshold value θ_{fc}. Consequently, when averaged over the depth Z_r, the dynamics of soil water in the above model operate identically to the stochastic soil water models cited earlier, so long as the correct parametrization of the loss processes are adopted, as described in the model development above. This approach allows us to make use of results derived by *Botter et al.* [2007], who used a similar approach to examine controls on the pdf of base flow. In that work the behavior within the vadose zone was not considered, but an expression was derived for the mean frequency with which the storage capacity of the vadose zone

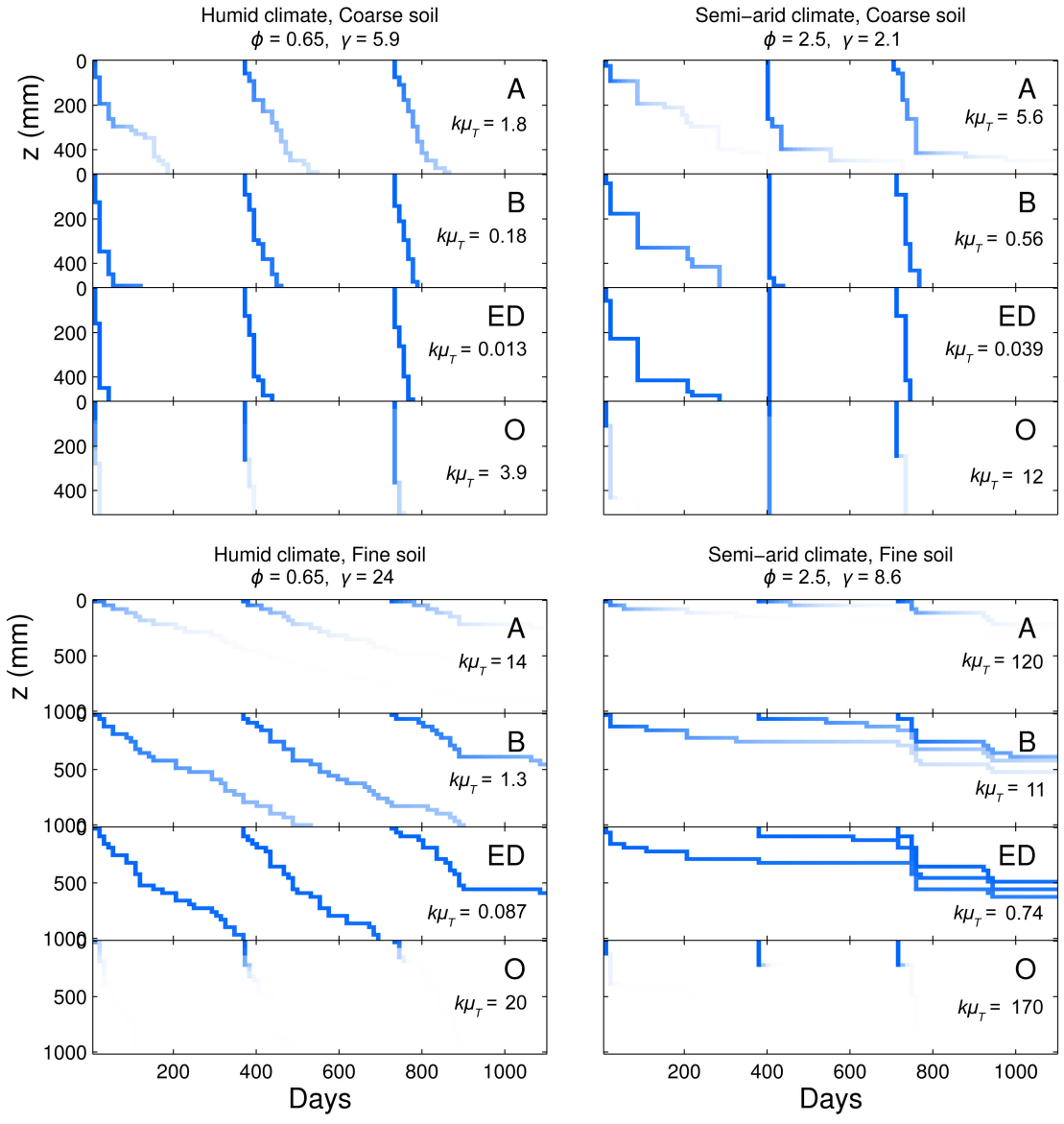

Figure 2. Typical transport and degradation of four pesticides in coarse and fine soils under a humid climate and a semiarid climate, as given by the parameters in Tables 1, 2, and 3. As the pesticides move down through the soil profile, they are degraded (indicated by the fading lines) and spend more time at a particular depth before being mobilized by the flow again and "jumping" to a deeper point or being leached out of the domain. See text for definitions of the dimensionless numbers given.

was exceeded, and a recharge event was triggered. This expression essentially expresses the recharge event series as a censored version of the infiltration event series. Here this expression plays a critical role. Furthermore, we will assume that the distribution of infiltration events is unbounded, (corresponding to the $r \gg 1$ case analyzed by *Botter et al.* [2007]).

[41] To proceed, we note that the paths traced by the solutes in Figure 2 appear to have the form of a random walk with strictly positive jump sizes. The jumps $\{\zeta_i\}$ are the transport events driven by infiltration past each depth. The intervals between jumps $\{\tau_i\}$ are the waiting times between transport events. To obtain the pdf of travel times through the vadose zone, it is therefore necessary to determine the appropriate distributions for the jump sizes $f_\zeta(\zeta)$ and waiting times $f_\tau(\tau)$.

[42] Unlike previous random walk approaches [*Jury and Gruber*, 1989; *McGrath*, 2007], the distribution of jumps and intervals in the transport through the vadose zone may not be independent of the position ξ_j in the profile. The variations in the distributions with depth are bounded at the surface by the distribution of infiltration events and at the base by the distribution of leaching events from the vadose zone. The distribution at the base differs from that of the surface because of the soil water deficits created by the evapotranspiration of soil water between events.

[43] Recent work provides a basis for developing expressions for these distributions. *Porporato et al.* [2004]

showed that these dynamics are a function of just two dimensionless parameters, which we will use here to express the required results. Recast here in a convenient form, the first is the aridity index ϕ and is the ratio of the maximum evapotranspiration rate and the rainfall rate:

$$\phi = \frac{\mathrm{ET}_{\max}}{\alpha \lambda_p}. \tag{15}$$

[44] The second is γ, the ratio of the potential range of storage in the vadose zone $(Z_r(\theta_{fc} - \theta_{pwp}))$ and the average depth of the storm events (α):

$$\gamma = \frac{Z_r(\theta_{fc} - \theta_{pwp})}{\alpha}. \tag{16}$$

[45] It can be shown that the magnitudes of the drainage events will follow the same exponential distribution as the infiltration events [*Botter et al.*, 2007; *Rodriguez-Iturbe et al.*, 1999]. This effect is related to the "memoryless" property of the exponential distribution. For an exponentially distributed set of random variables X, the pdf of $X - c$ for all $X > c$ is identical to the pdf of X. Another way to express this is that the conditional probability $P(X > x|X > c)$ is equal to the probability $P(X > x - c)$ for $x > c > 0$ when X is an exponentially distributed random variable. In essence, the effect of the unsaturated zone is simply to alter the frequency of events (filtering those events that are $< c$ in the previous example) but not their magnitude. If this is the case, the distribution of jump sizes $f_\zeta(\zeta)$ can be found simply by noting that the transport of the solutes depends on the pore volume participating in transport $(\theta_{fc} - \theta_r)$ and the retardation factor (as given in equation (12)) such that

$$f_\zeta(\zeta) = \frac{RF\gamma}{Z_r} \exp\left(-RF\gamma \frac{\zeta}{Z_r}\right). \tag{17}$$

[46] This result is very powerful and simplifies the analysis. Here $F = (\theta_{fc} - \theta_r)/(\theta_{fc} - \theta_{pwp})$ is a factor relating the fraction of pore volume that participates in advective transport to the fraction that evapotranspiration is extracted from. Note that nonphysical results can occur if $\theta_r > \theta_{pwp}$, such as transport beyond the base of the wetting front, so we require $F > 1$. For convenience we can treat the product RF as a single variable in much of what follows since these factors always appear together, and we will refer to this as the "adjusted retardation factor."

[47] *Botter et al.* [2007] also derived an expression for the mean of the waiting times between leaching events based on the assumption that infiltration at the surface follows a marked Poisson process with an exponential distribution of event magnitudes. *McGrath et al.* [2007] further derived expressions for the first n moments of the waiting time distribution between leaching events. From these the mean rate of leaching events can be derived as

$$\lambda_d = \lambda_p \frac{e^{-\gamma} \gamma^{\frac{\gamma}{\phi}} \phi / \gamma}{\Gamma\left(\frac{\gamma}{\phi}\right) - \Gamma\left(\frac{\gamma}{\phi}, \gamma\right)}, \tag{18}$$

where $\Gamma(a)$ is the gamma function and $\Gamma(a, z)$ is the incomplete gamma function [*Abramowitz and Stegun*, 1972].

[48] *Botter et al.* [2007] suggested that when the ratio γ/ϕ is sufficiently small (they suggest less than 0.1, though this value is unrealistically small for most applications), the distribution of waiting times between recharge events can be approximated by an exponential distribution with a rate parameter λ_d. *McGrath et al.* [2007] observed that for larger γ/ϕ (called β in their notation) the distribution of waiting times becomes less and less like a exponential distribution and instead exhibits a clustering behavior that is amplified when ϕ is close to 1. This clustering arises from the increased probability of short waiting times when the soil water content is close to the maximum capacity and more likely long waiting times when soil water content is low.

[49] Numerical tests were conducted using the model for a variety of values of γ and ϕ to determine the validity of assuming an exponential distribution of jump sizes and waiting times. Figure 3 strongly supports the assumption that the jump sizes are, in fact, exponentially distributed throughout the profile with a mean given by $\alpha/[R(\theta_{fc} - \theta_r)]$. However, Figure 4 suggests a more complex picture for the waiting time distribution. For humid climates ($\phi < 1$) and very small γ (<1) the distribution does appear to follow an exponential distribution with rate constant λ_d (given by the blue line). Such small values of γ have little physical significance since they represent unrealistically small rooting zones. However, in deeper and drier soils this approximation does not hold, particularly in the deeper parts of the soil. The shorter waiting times seem to follow an exponential distribution with the same arrival rate as the infiltration λ_p. However, the tail of the distribution appears to follow a power law with an exponent that decreases deeper in the profile and as γ and ϕ increase.

[50] Proceeding toward an analytical derivation of the pdf, these results suggest that an exponential distribution of

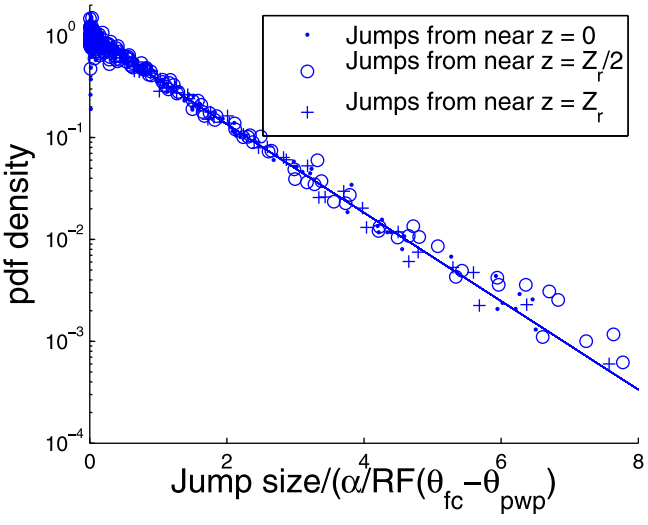

Figure 3. Transport distance in each jump (see Figure 2) follows an exponential distribution with a mean given by $\alpha/R(\theta_{fc} - \theta_r)$. This appears to hold throughout the profile and for all combinations of γ and ϕ (the results for multiple scenarios are plotted here; all plot on top of each other).

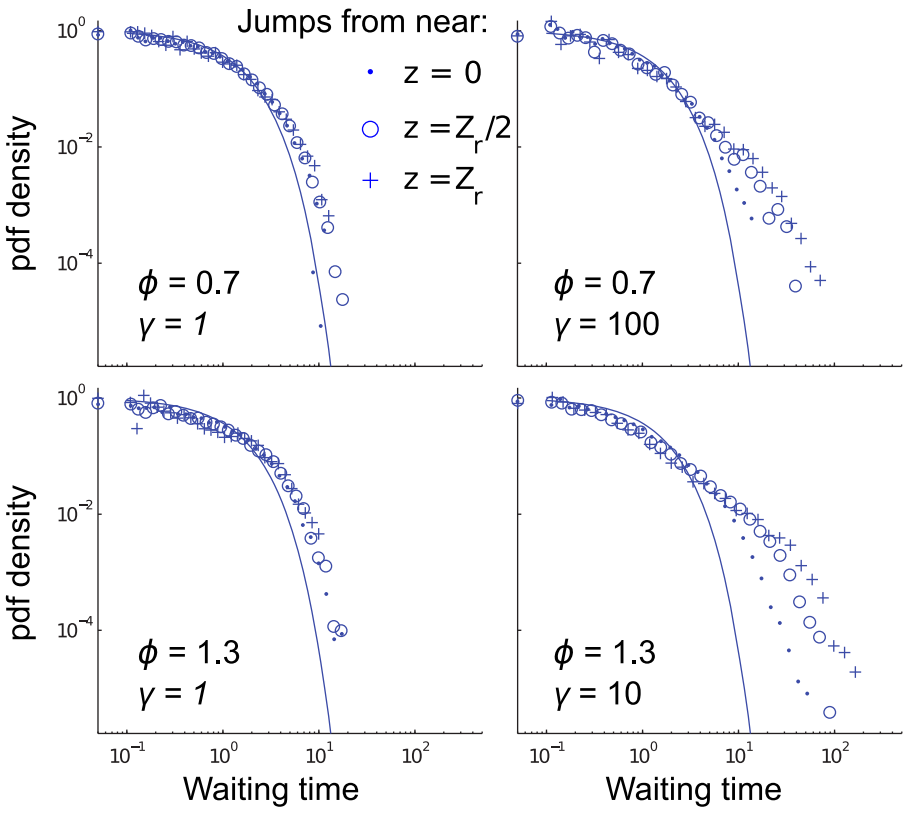

Figure 4. Numerical experiments indicate that the waiting times between transport events do not follow an exponential distribution except for when γ and ϕ are small. They also become increasingly power law with depth. The solid line gives the pdf of the waiting times between infiltration events (an exponential with rate parameters λ_p).

jump sizes is justified for this model but that the assumption of an exponential distribution of waiting times may lead to inaccurate results in some cases.

3.2. Framework for Deriving the PDF of Transit Times and Delivery Ratios

[51] In the interest of obtaining an analytical result we will assume that the water flux past a point ξ is a Poisson process with the same mean volume throughout the profile but a rate that depends on the depth $\lambda(\xi) \leq \lambda_p$. Under these conditions we can make the following arguments to derive the pdf of travel times T through the vadose zone. Wetting fronts enter the vadose zone and traverse it in a series of independent steps that are drawn from an exponential distribution with parameter $\alpha/[R(\theta_{fc} - \theta_r)]$. From the properties of such a process, we can say that the number of steps n required for a front to reach the base is given by a Poisson distribution with parameter $RF\gamma$, and the position ξ of a step is uniformly distributed throughout the column.

[52] Note that the probability that the front takes exactly zero steps to reach the base is equal to $\exp(-RF\gamma)$. This is the probability that an event will completely "flush" the system, transporting the new wetting front and all the solute fronts stored in the vadose zone through the reference plane at the base of the vadose zone. Furthermore, when R is large, the probability that the solute will reach the base in a finite amount of time approaches zero.

[53] The waiting time for any particular step τ_i can be found by randomizing the value of ξ in the wetting front arrival rate according to a uniform distribution on $[0, Z_r]$:

$$f_{\tau_i} = \frac{1}{Z_r}\int_0^{Z_r} \lambda(\xi) e^{-\lambda(\xi)\tau_i} d\xi. \tag{19}$$

[54] If $n - 1$ steps are required to traverse the vadose zone, then the total travel time T_n is the sum of the $n - 1$ values of τ_i. The distribution of the sum of n random variables is given by the n-fold convolution of the pdf of each value:

$$f_{T_n} = \left(\underbrace{f_{\tau_i} * f_{\tau_i} * \cdots * f_{\tau_i}}_{n}\right)(T_n), \tag{20}$$

where the asterisk is the convolution operator. Finally, the number n is itself a random variable with a Poisson distribution with parameter $RF\gamma$. To obtain the distribution of the travel times T, we must therefore randomize the value of n in the distribution of the n-step travel time f_{T_n}.

$$f_T(T) = \sum_{n=0}^{\infty} f_{T_n} \frac{e^{-RF\gamma}(RF\gamma)^n}{n!}. \tag{21}$$

[55] These steps can be followed to obtain a pdf of T so long as (1) the function $\lambda(\xi)$ can be specified, (2) closed

forms of the integrals can be found, and (3) a form for f_{T_n} can be found for arbitrary n. Each of these steps represents a considerable mathematical challenge, and it is likely that closed form analytical solutions will be achieved for only a handful of cases.

[56] *Laio et al.* [2006] developed a vertically extended stochastic soil water content model to predict how the pdf of soil water content varies with depth. They derived a general expression for $\lambda(z)$ and an explicit solution for the case of a uniform root profile. However, this expression could not be carried through the above steps to produce an analytical solution for $f_T(T)$. In section 3.3 we derive an analytical expression for when $\phi = 0$ and an approximate solution for $\phi \neq 0$.

3.3. Analytical Solution for $\phi = 0$

[57] One case where an analytical solution can be found is where there is no evapotranspiration. In that case, the storage deficit is always zero, and the same amount of water flows past every point in the profile, so the function describing the mean waiting time at a given depth $\lambda(\xi)$ is constant at $\lambda(\xi) = \lambda_p$. Thus, f_{τ_i} is simply an exponential distribution with parameter λ_p. The sum of n independent, identically distributed exponential random variables is given by a gamma distribution with a shape parameter n and a scale parameter equal to the rate constant of the underlying exponential distribution. Therefore, we can determine the pdf of the amount of time T each solute front spends in the vadose zone by randomizing the shape parameter of a gamma distribution according to the Poisson distribution, as given above. This yields

$$f_T(T) = \begin{cases} \dfrac{\exp(-RF\gamma - T\lambda_p)}{T}\sqrt{T\lambda_p RF\gamma}\, I_1\left(2\sqrt{T\lambda_p RF\gamma}\right) & T > 0 \\ \exp(-RF\gamma) & T = 0 \end{cases}, \tag{22}$$

where $I_1(z)$ is the modified Bessel function of the first kind. The pdf of *Jury and Gruber* [1989] differs from that presented here in that they assume a gamma distribution of infiltrating volumes (rather than exponential) and account for the waiting time between solute application and the first storm. In this distribution, λ_p operates as scale parameter, and $RF\gamma$ controls the shape of the distribution. When $RF\gamma$ is close to 1, many of the events have $T = 0$, and the distribution for $T > 0$ drops off quickly. When $RF\gamma$ is larger, it becomes increasingly symmetrical, approximating a normal distribution. The mean and variance of the distribution are given by

$$\mu_T = \frac{RF\gamma}{\lambda_p}, \quad \sigma_T^2 = \frac{2RF\gamma}{\lambda_p^2}. \tag{23}$$

[58] These moments can be derived as a special case of the pdf derived by *Jury and Gruber* [1989] when the waiting time between solute application and the first storm is neglected [see *McGrath*, 2007].

[59] If the fronts carry a solute subject to first-order degradation, then the proportion of mass remaining when the front exits the system to the initial mass M/M_0 (which we shall refer to as the delivery ratio, DR) is a function of the transit time T and the degradation rate constant k (equation (14)). Since T is a random variable, DR is also a random variable, and since the pdf of T is known (under the approximations given above), we can also determine the pdf of DR. In general, if a random variable Y is a monotonically decreasing function $y = g(x)$ of another random variable X, then their distributions $f_Y(y)$ and $f_X(x)$ are related by

$$f_Y(y) = -f_X\left[g^{-1}(y)\right]\frac{\mathrm{d}[g^{-1}(y)]}{\mathrm{d}y}, \tag{24}$$

where $x = g^{-1}(y)$. Here equation (14) is g, and equation (22) is f_X. Thus, we can find the pdf of DR as

$$f_{\mathrm{DR}}(\mathrm{DR}) = {}_0\tilde{F}_1\left(2, -\frac{RF\gamma}{k_d/\lambda_p}\log(\mathrm{DR})\right)\frac{RF\gamma}{k_d/\lambda_p}e^{-RF\gamma}\mathrm{DR}^{\frac{1}{k_d/\lambda_p}-1} \tag{25}$$

plus an atom of probability at DR = 1 equal to $\exp(-RF\gamma)$, corresponding to the events that flush the solute all the way through the soil. The function ${}_0\tilde{F}_1$ is the regularized confluent hypergeometric function [*Abramowitz and Stegun*, 1972]. The nth raw moment of the delivery ratio is given by

$$\mu_n = \exp\left(-\frac{RF\gamma n k_d}{\lambda_p + nk_d}\right), \tag{26}$$

so that the mean and variance are given by

$$\mu_{DR} = \exp\left(-\frac{RF\gamma k_d}{\lambda_p + k_d}\right) \tag{27}$$

$$\sigma_{DR}^2 = \exp\left(-\frac{2RF\gamma k_d}{\lambda_p + 2k_d}\right) - \exp\left(-\frac{2RF\gamma k_d}{\lambda_p + k_d}\right). \tag{28}$$

3.4. Approximate Solution for $\phi > 0$

[60] When $\mathrm{ET}_{\max}$ is not zero ($\phi > 0$), the storage deficit created by evapotranspiration will reduce the frequency with which wetting fronts reach a depth z in the soil, leading to the more complex distributions shown in Figure 4. However, it is possible that effective values of the mean waiting time between transport events λ_e and shape parameter $RF\gamma_e$ can be found. Here we explore this possibility by comparing the analytical results obtained above to HEIST. By rearranging the expression for the mean and variance of the travel time we can obtain expressions to infer the effective parameter values:

$$\lambda_e = \frac{2\mu_T}{\sigma_T^2}, \tag{29}$$

$$\gamma_e = \frac{2\mu_T^2}{RF\sigma_T^2}. \tag{30}$$

[61] The numerical model was run for 400 combinations of random soil and climate parameters to ensure that the effective parameter gave reasonable results over the full parameter range. The adjusted retardation factor was set at 1. All parameters were sampled independently to ensure maximum coverage of the parameter space. Rainfall parameters were sampled from distributions fitted to the data of *Hawk*

and Eagleson [1992]. ET_{max} was sampled from a gamma distribution with a mean of 1000 mm and standard deviation of 500 mm. Soil depths Z_r were sampled from a log-normal distribution with a scale parameter of 1 m and a shape parameter of 2.5. Soil properties were obtained by choosing percent sand uniformly from 0 to 100% and percent clay uniformly from 0 to the minimum of 20% or 100% minus percent sand. Field capacity and wilting point were assumed to correspond with the water contents at 33 and 1500 kPa obtained from the pedotransfer functions of *Saxton and Rawls* [2006].

[62] It was found that the effective parameters inferred from the numerical results showed consistent and simple relationships with the ratio of the rate of leaching events λ_d derived by *Botter et al.* [2007] and the rate of infiltration events λ_p (Figure 5). The effective jump rate λ_e is very close to λ_d. The effective γ_e varies in a way that is very close to

$$\frac{\gamma_e}{\gamma} = \left(\frac{\lambda_d}{\lambda_p}\right)^{\frac{1}{2}}. \tag{31}$$

[63] These relationships are remarkably simple and suggest that it may be possible to derive closed form analytical solutions for the travel time distribution that do not rely on these approximate relationships. It is curious to note that the effect of the censoring of infiltration events at depth is to reduce both the effective rate of jumps from λ_p to λ_d and their effective size by reducing γ. This is despite the fact that numerical results presented here (Figure 3) and in the work by *Botter et al.* [2007] suggest that the actual jump size distribution is unchanged by the storage deficit censoring. Hopefully, this paradoxical result can be resolved in the future by a more complete analytical treatment of the problem.

[64] We would like to be able to use these effective parameters in the expressions for the pdf and moments of the travel time and delivery ratio derived above. In using these effective parameters, it is necessary to consider the role of the atom of probability $\exp(-RF\gamma)$ that appears in the expression for the travel time and delivery ratio pdf's. These atoms refer to the case where a storm event flushes the solute load completely through the system and are therefore not affected by the antecedent soil water storage. The value of $RF\gamma$ used to calculate the probability of this occurrence should therefore not be replaced with the effective value $RF\gamma_e$. However, this creates an inconsistency in the pdf, such that its zeroth moment may not be unity. To correct this, we must introduce a correction C that scales the main part of the pdf:

$$C = \frac{1 - e^{RF\gamma}}{1 - e^{RF\gamma_e}}. \tag{32}$$

[65] This factor is slightly greater than 1 in most cases and can usually be neglected. It is only significant when ϕ and γ are both very large. By neglecting this factor we can, indeed, substitute the effective parameters into the expressions for the moments of the travel time distribution and delivery ratio derived for the case with $\phi = 0$.

[66] Figure 6 shows that the approximate analytical expressions provide an excellent prediction of the first two moments of the distribution. Figure 6 compares the sample mean and variance $\bar{T}$ and S_T^2 observed over many simulations to the mean and variance μ_T and σ_T^2 obtained from equation (23) using the original parameters, as well as those obtained by using the effective parameter values in (23). The results show that as would be expected, when $\phi > 0$, the original parameters significantly underestimate the

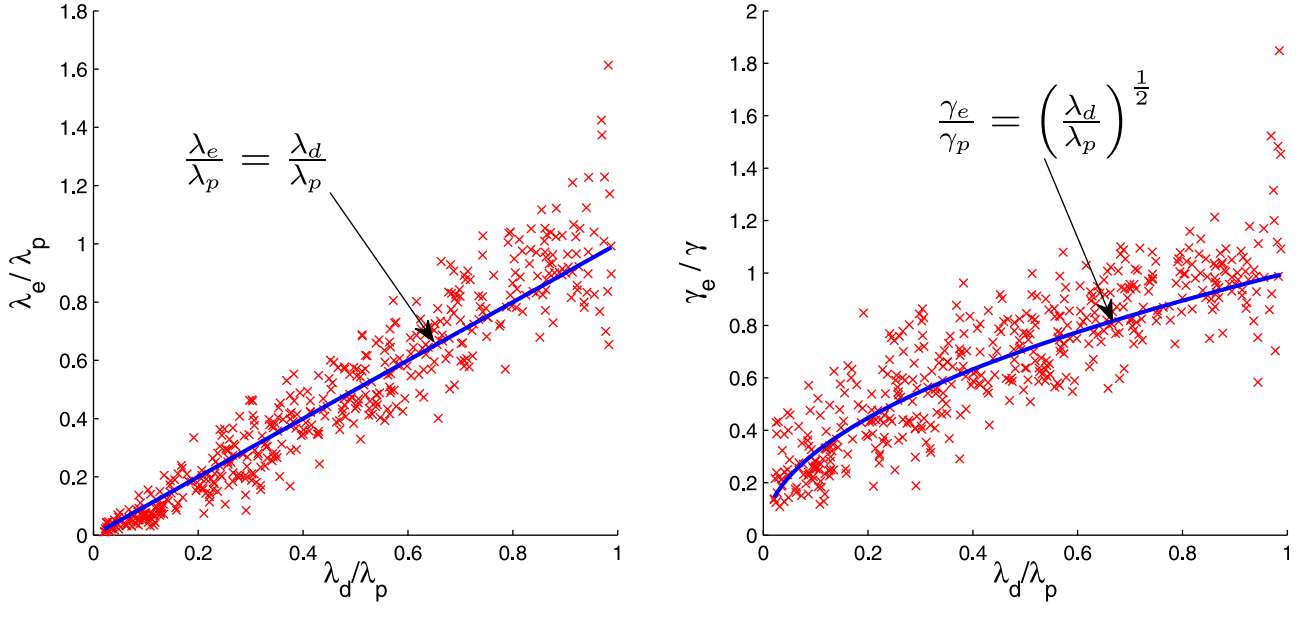

Figure 5. Relationships between the effective parameters observed in 400 random simulations (normalized by their original values) λ_e/λ_p and γ_e/γ and the ratio λ_d/λ_p. Two very simple relationships emerge: the effective mean jump rate λ_e is very closely approximated by λ_d, and the effective storage parameter γ_e scales with $(\lambda_d/\lambda_p)^{\frac{1}{2}}$.

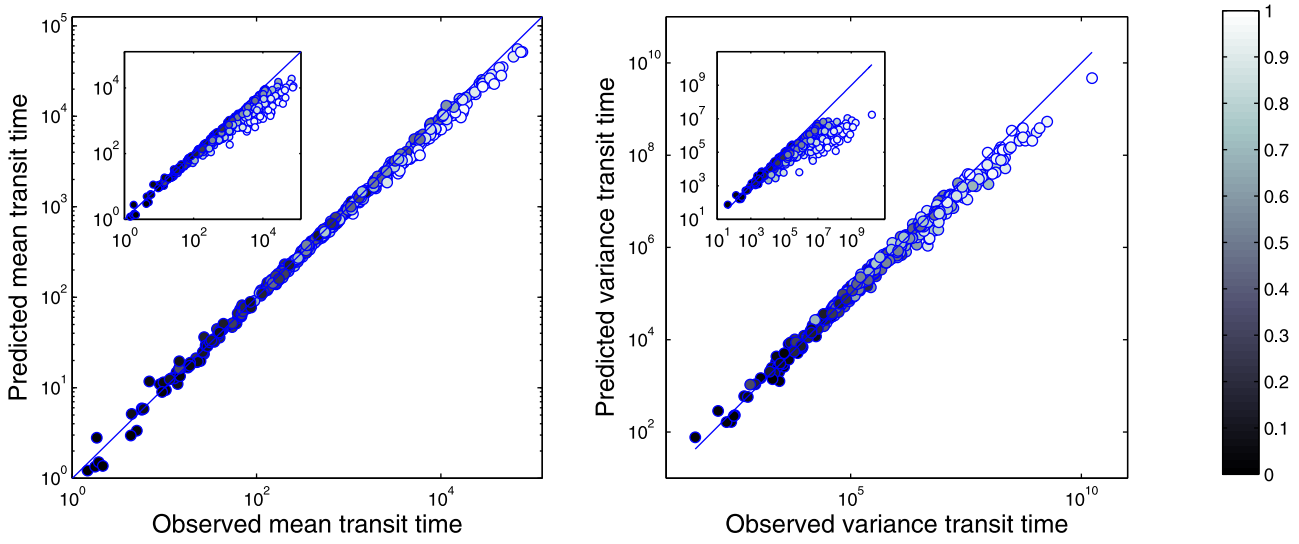

Figure 6. Comparison of mean and variance of the travel time distribution predicted by equation (23) with the parameters λ_p and γ replaced with the effective parameters λ_e and γ_e, with those derived from 400 random simulations. The inset plots show the same relationships without the correction. The water balance E/P in each simulation is represented by the tone of the dots. These results show that the moments of the travel time distribution are very well characterized by the derived expressions when the effective parameters are used.

mean and the variance of the age distribution. In such cases the reduction of the average load velocity due to evapotranspiration is not accounted for. The effects are strongest for the drier sites (light dots). On the other hand, the effective parameter values give an excellent prediction.

[67] Using the effective parameters in the pdf of the delivery ratio, equation (25), gives a very close match to the numerical results (Figure 7). These results show that the semianalytical solution obtained by using the effective parameters is able to correctly characterize the behavior of the numerical model over a wide range of conditions.

4. Discussion

4.1. Sensitivity to Climate and Soil Properties

[68] The numerical model and semianalytical result presented above suggest that the controls of climate, soils, and solute properties on the residence time and delivery ratio of solutes in the vadose zone have a remarkably simple relationship to the soil water balance. This can be seen by noting that λ_d/λ_p is simply the ratio of the mean rate of recharge from the base of the soil ($\alpha\lambda_d$) to the mean infiltration at the surface (α/λ_p). Defining this recharge ratio as $\Omega = \lambda_d/\lambda_p$, the effective parameters determined above can then be defined relative to their original values as $\lambda_e = \lambda_p\Omega$ and $\gamma_e = \gamma\sqrt{\Omega}$. Alternatively, $\Omega = (1 - H)$, where H is the local value of the Horton index $\mathrm{ET}/\alpha\lambda_p$ [*Troch et al.*, 2009], the ratio of evapotranspiration and infiltration. Second, we define κ as the ratio of the degradation rate and the frequency of storms k_d/λ_p. With these ratios and assuming $C \sim 1$, we can rewrite the moments of the travel time and delivery ratio as

$$\mu_T = \frac{RF\gamma}{\lambda_p}\Big/\sqrt{\Omega}, \tag{33}$$

$$\sigma_T^2 = \frac{2RF\gamma}{\lambda_p^2}\Big/\left(\sqrt{\Omega}\right)^3, \tag{34}$$

$$\mu_{DR} = e^{-\frac{RF\gamma\kappa\sqrt{\Omega}}{\kappa+\Omega}}, \tag{35}$$

$$\sigma_{DR}^2 = e^{-\frac{2RF\gamma\kappa\sqrt{\Omega}}{2\kappa+\Omega}} - e^{-\frac{2RF\gamma\kappa\sqrt{\Omega}}{\kappa+\Omega}}. \tag{36}$$

[69] Note that we can express the moments of the travel time as the product of a "wet travel time" μ_{T0}, which is the travel time when there is no evapotranspiration, and a deceleration factor, which is simply $\Omega^{-1/2}$, that accounts for the effect of evapotranspiration, giving $\mu_T = \mu_{T0}\Omega^{-1/2}$. Similarly, for the variance, $\sigma_T^2 = \sigma_{T0}^2\Omega^{-3/2}$. In other words, the travel time predicted by this model $\mu_{T0}/\sqrt{\Omega}$ is simply the geometric mean of the travel time predicted by the mean infiltration rate μ_{T0} and that predicted by the mean leaching rate μ_{T0}/Ω. It is common in simple pesticide risk analysis to estimate mean travel time using a mean leaching rate calculated from the water balance [*Rao et al.*, 1985b; *Wang et al.*, 2009]. According to the simple model presented here, this travel time is an overestimate by a factor of $1/\sqrt{\Omega}$ because it does not account for the relatively rapid transport through the upper part of the profile.

[70] The value of $\Omega^{-1/2}$ is shown in Figure 8 as a function of the dimensionless numbers γ and ϕ. For small γ, which represents shallow soils and large infiltration events, the effects of ET are minor, as the soil water storage is not large enough (compared to the average storm depth) for the antecedent soil water conditions to have a significant control. In humid systems ($\phi < 1$), the effects are also small and become insensitive to variations in larger values of γ. In these cases, the potential for water to be removed by evapotranspiration between storms is generally less than

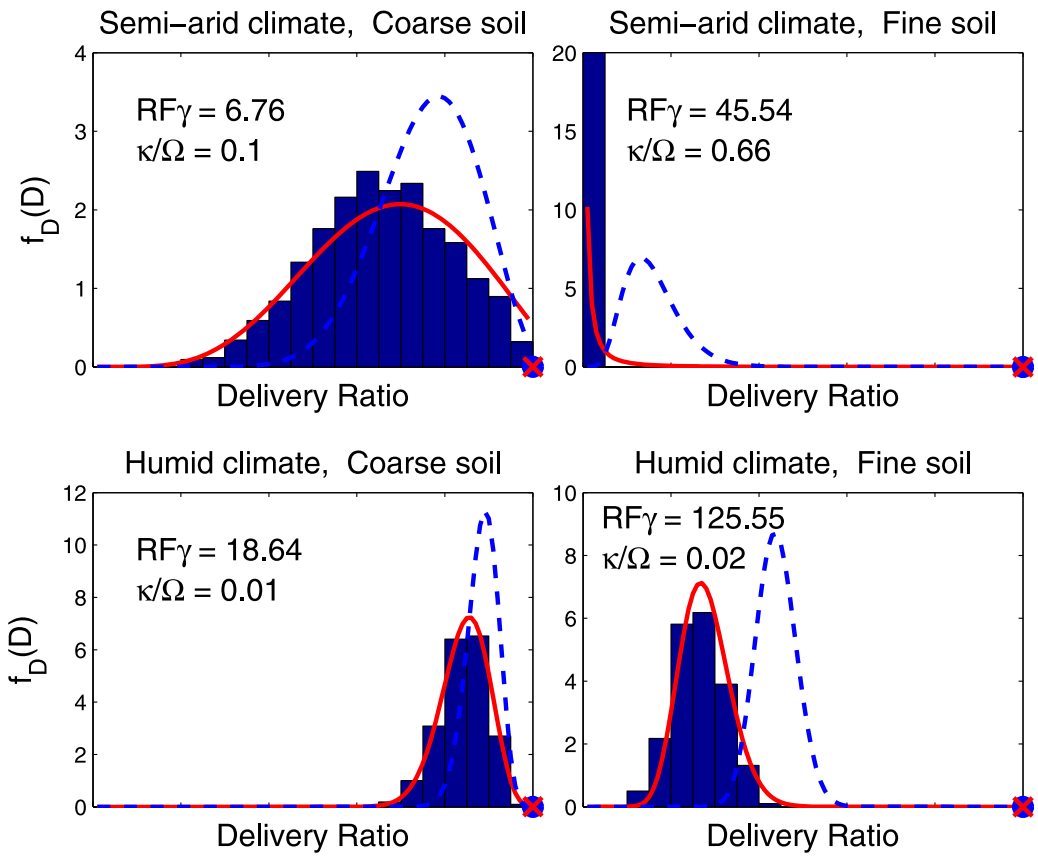

Figure 7. Examples of the ability of equation (25) to predict the pdf of the delivery ratio for bromacil. When the original parameters are used, representing the case with no evapotranspiration, the delivery ratio is overestimated (dashed line). When evapotranspiration is accounted for using the effective parameters, equation (25) provides an excellent prediction of the pdf of pesticide delivery (solid line).

the size of the storm events, and so most (but not all) storms bring the soil profile to field capacity and initiate drainage. In more arid systems ($\phi > 1$), however, the system can dry out between storms. The accumulated infiltration from a closely spaced run of multiple storms is required to initiate drainage. For larger values of γ (that is, thicker soils or smaller storms), the total depth of infiltration required to transport the solute load to the base increases, and the recharge ratio decreases, and so μ_T and σ_T increase.

[71] We can visualize the effect of evapotranspiration on the travel time by plotting contours of the mean and coefficient of variation (CV) of the travel times, normalized so that they are functions of only γ and ϕ: that is, $\lambda_p \mu_T / RF = \gamma/\sqrt{\Omega}$ and $\sqrt{RF}\sigma_T/\mu_T = \sqrt{2/(\gamma\sqrt{\Omega})}$ (Figure 9). The normalized mean increases with γ and with the effect of $\Omega^{-1/2}$ shown in Figure 8. In humid climates the relative variability of the travel time decreases with larger γ. When γ is small (shallow soils or large storms), the mean travel time is insensitive to climate and depends only on γ. In these cases the flushing events are important, and the initial soil moisture conditions have limited effect on the travel time. For higher γ in humid climates ($\phi < 1$), Ω approaches 1, the water balance effects on travel time are small, and the travel time is still mainly a function of γ. However, in dry climates the recharge ratio Ω becomes small, and so $\Omega^{-1/2}$ becomes very large, and the travel time rapidly climbs.

[72] For small γ the soil moisture conditions have little effect, and so variability in travel time is controlled by the variability in the rainfall (consistent with the findings of *Foussereau et al.* [2001]. Because the rainfall is here assumed to be a Poisson process, the CV of T is close to 1 (this is a property of the exponential distribution of interstorm periods). For large γ in humid climates ($\phi < 1$) the transit of a point load through the deeper soil requires many infiltration events. The variability of waiting times between these individual events is averaged out in the total (law of large numbers), and so the CV of the total travel time declines. In contrast, in more arid areas the variability in T increases greatly for increasing γ. In these cases, recharge that is able to exceed the storage deficit is simply so rare that solutes remain in the soil for very long periods and their travel time is determined by (highly variable in time) rare events.

[73] Extending this discussion to the delivery ratio, the delivery is largely determined by the Damköhler number [*Domenico and Schwartz*, 1990; *Ocampo et al.*, 2006; Rao et al., submitted manuscript, 2010], which captures the relative rates of reaction to transport. Here these are given by $Da = k_d \mu_T$ and $Da_0 = k_d \mu_{T0}$ for the cases with and without

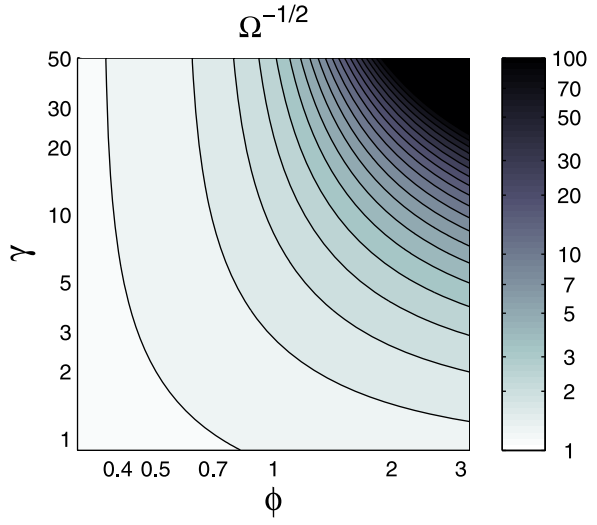

Figure 8. Contours $\Omega^{-1/2} = \sqrt{\lambda_p/\lambda_d}$ as a function of the soil ratio γ and the aridity index ϕ. This function of the water balance controls the increase in travel time due to the effect of evapotranspiration. A note on interpretation is the following: since α appears in the denominator of the definitions of both γ and ϕ, an increase in storm depth alone would mean decreasing both γ and ϕ (i.e., move the system toward the bottom left of this plot) and increasing the recharge ratio Ω. Alternatively, if climate change led to an increase in the intensity of storms without changing the total annual rainfall, implying a compensating decrease in λ_p and a constant ϕ, the increase in Ω would come from a decrease in γ alone.

evapotranspiration, respectively. A front moving at the average rate will have a delivery ratio given by $\mu_{DR} = \exp(-k_d\mu_T) = \exp(-Da)$. The expression for the mean delivery ratio given in equation (35) reduces to this when $\kappa/\Omega \ll 1$, that is, when degradation rates are slow compared with the leaching rate. This critical ratio can also be written as k_d/λ_d. However, when degradation rates are large ($\kappa/\Omega \gg 1$), the mean delivery ratio is given by $\mu_{DR} = \exp(RF\gamma\sqrt{\Omega})$, which is closely related to the probability that a rainfall event will "flush" the vadose zone and carry the solute from the surface to the base in a single event.

[74] We can see this dependence in a contour plot of the mean and variance (as functions of ϕ and γ, equation (35)) of the delivery ratio for fixed values of κ and RF (Figures 10 and 11). When κ is 1 (Figures 10, top, and 11, top), indicating a degradation rate similar to the rate of storm interarrivals, the delivery ratio is small, and there is low sensitivity to ϕ. In these cases, κ will always be larger than 1, and so the delivery ratio is close to zero except for those times where there is an event that flushes the whole soil column. Therefore, the average delivery ratio depends primarily on γ since this parameter controls the frequency of the flushing events. The variance is greatest for those values of γ where the mean is changing most rapidly with respect to γ, which is around 1 for $RF = 1$ and around 3 for $RF = 3$.

[75] When κ is small (Figures 10, bottom, and 11, bottom), the product κ/Ω can be less than 1 provided that the recharge ratio is not too small. Consequently, the delivery ratio tends to be larger and more strongly dependent on the climate. In these cases the ability of evapotranspiration to effectively slow down the transport of a solute through the vadose zone (and thus increase μ_T) becomes important. For a value of γ around 10, the delivery ratio at a humid site (say $\phi = 0.3$) will be around 90% on average, while at an arid site ($\phi = 3$) it will be close to 0%. The variance tends to be smaller for small κ than for $\kappa = 1$ but is also greatest for the regions where the mean is changing rapidly with γ. It tends to increase with ϕ.

4.2. Classification of Realistic Scenarios

[76] The framework presented here is useful for interpreting and classifying the different controls on travel times and help us to better understand the scenarios presented in section 2.3. Table 4 shows the value of various dimensionless numbers calculated from the parameters of the example scenarios. Figures 12 and 13 show the mean and standard deviation of the transit time and delivery ratio for the example scenarios calculated both numerically and with the analytical solutions. Travel times range from a few

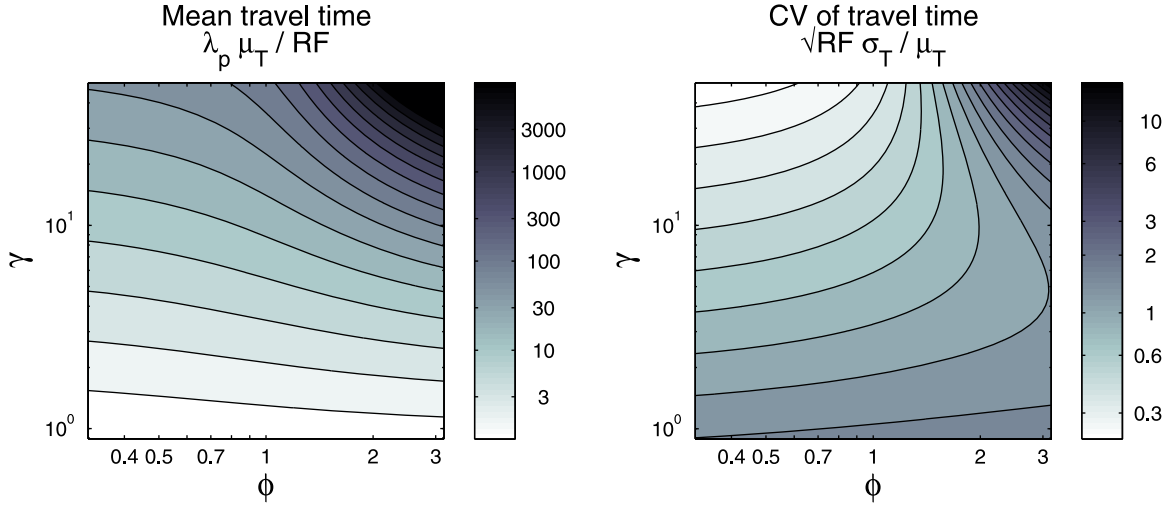

Figure 9. Contours of the normalized mean and coefficient of variation (CV) of the arrival time distributions as a function of γ and ϕ. Darker colors represent larger values.

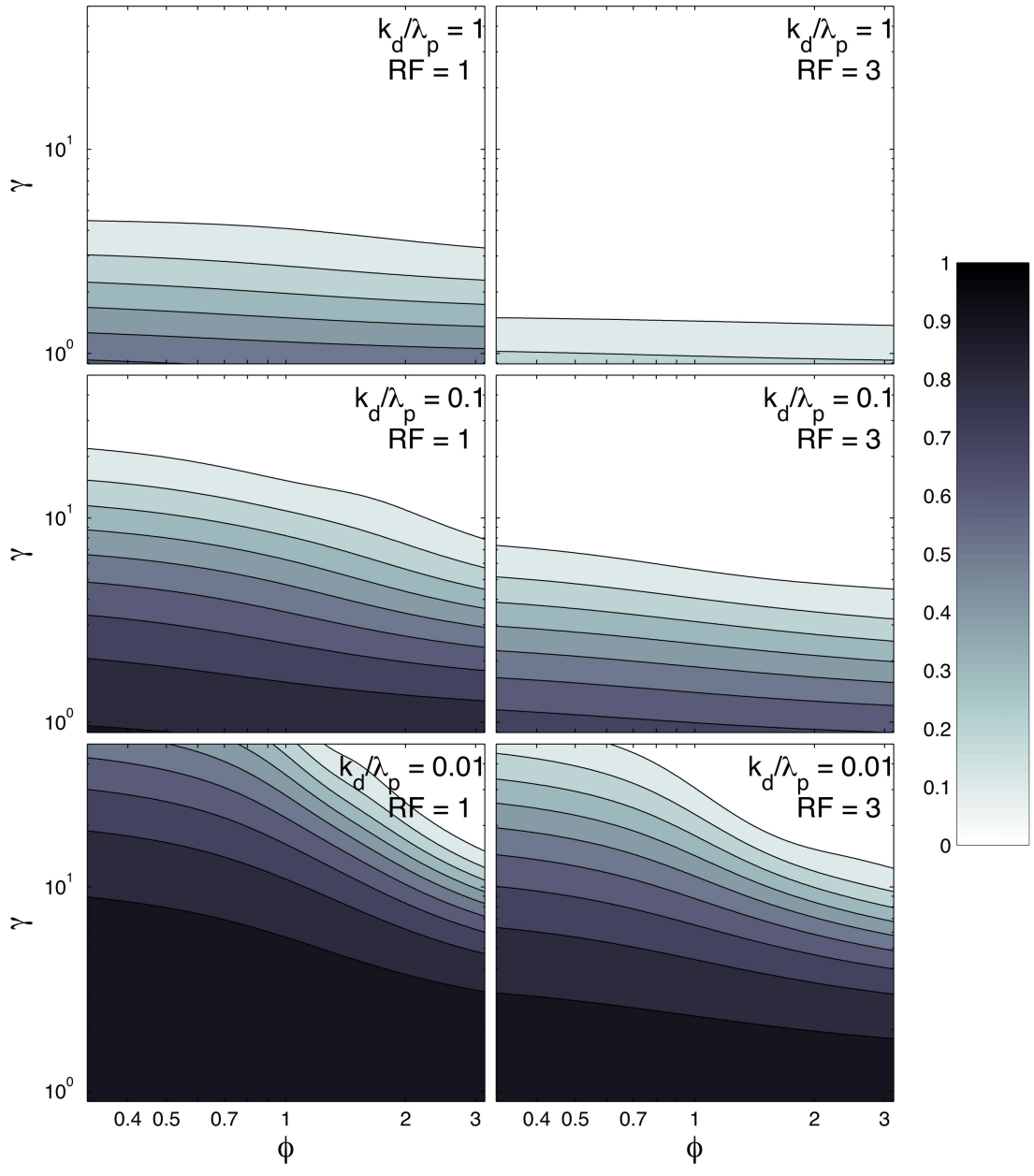

Figure 10. Contours of mean delivery ratio $< M/M_0 >$ as a function of ϕ and γ for various values of the adjusted retardation coefficient *RF* and normalized decay rate κ.

months in the coarse humid case to many years in the fine arid soil. In any climate the delivery ratio can vary from close to 0 to close to 1, depending on the retardation and reaction rates of the solute.

[77] We can classify these scenarios on the basis of whether the mean delivery ratio is primarily controlled by the mean travel time (when $\kappa/\Omega < 0.5$) or by the flushing events (when $\kappa/\Omega > 2$) or by a combination of both $0.5 < \kappa/\Omega < 2$ (the choice of 0.5 and 2 is somewhat arbitrary). We will refer to these as mean time limited, fast time limited, and colimited cases, respectively.

[78] The slowly degrading compounds bromacil and ethylene dibromide tend to be mean time limited, apart from bromacil in the fine, dry case, which is colimited. In contrast, oxamyl tends to be fast time or colimited because of its rapid degradation rate. Atrazine exhibits all three classes of behavior depending on climate and soil type. Mean time limitation is more common in the humid climate. In the dry climate the coarse soil tends to produce more mean-limited behavior, and the fine soil produces more fast-limited behavior.

[79] The actual delivery ratios that occur in these scenarios depend on the transit time and/or flushing probability. The numerical model predicts mean transit times varying from 34 days for weakly sorbing oxamyl in the coarse, humid case to 24 years for atrazine in the fine soil, dry climate case. The difference from the case with no evapotranspiration is a factor of about 1.5 in the first case to more than 4 in the second. The latter case has a large degree of variability, on the order of 4.3 years, though in relative

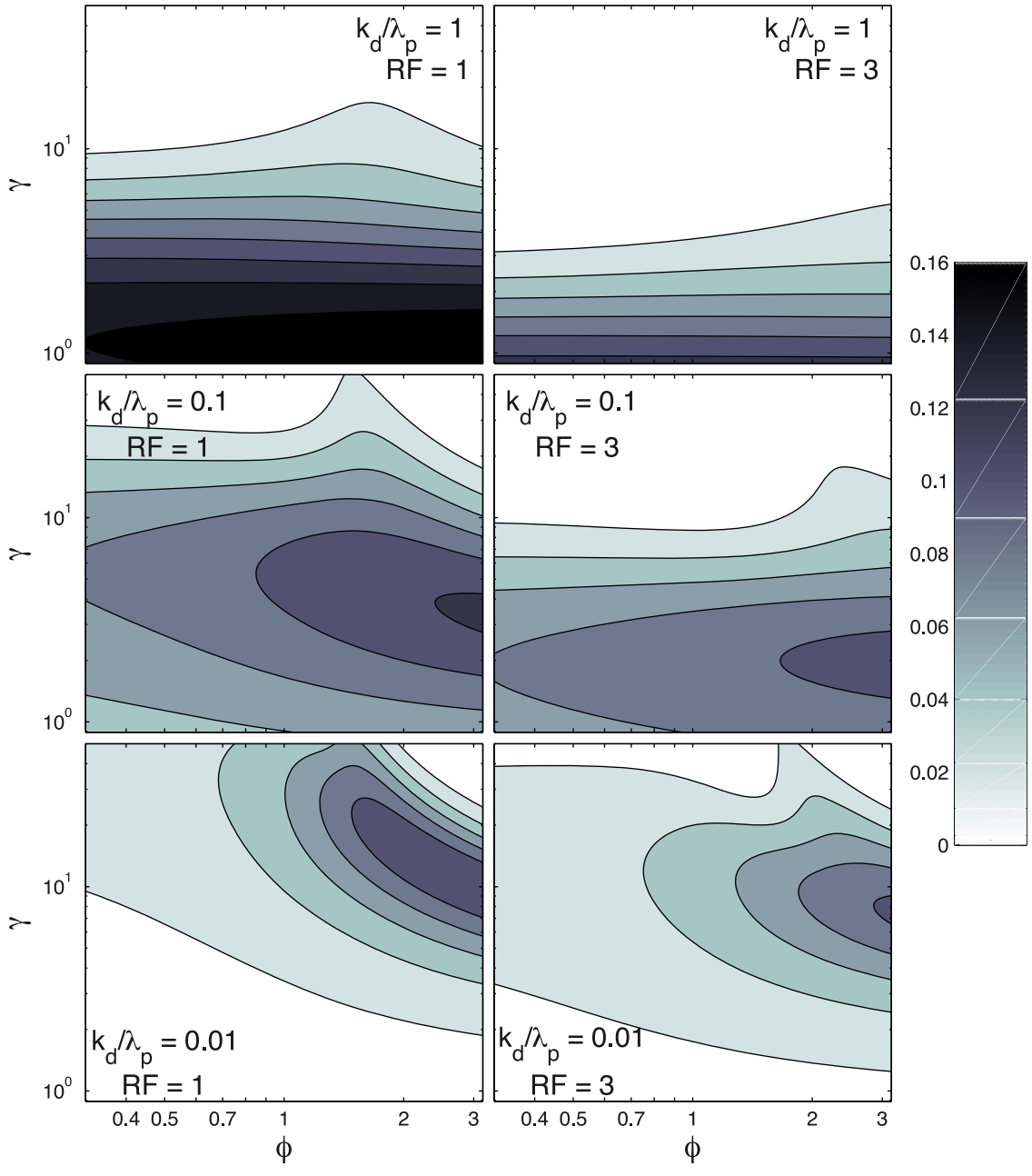

Figure 11. Contours of the variance of delivery ratio as a function of ϕ and γ for various values of the adjusted retardation coefficient *RF* and normalized decay rate κ.

terms this is less than 20% of the mean travel time. The largest relative variability occurs for oxamyl in the coarse dry case, where the relatively small value of $RF\gamma$ (4.6) means that flushing events are relatively common (about 1% of storms, compared to 1 storm in 10,000 for ethylene dibromide in the same soil and climate). The large value of κ/Ω (9.4) also suggests that these events control the expected delivery ratio.

5. Conclusions

[80] In this work we have used a range of modeling approaches to gain insight into the control of evapotranspiration on the travel time and delivery of reactive solutes through the vadose zone. A simple piston displacement model of 1-D retarded, reactive solute transport through a homogeneous soil profile was implemented and compared to HYDRUS 1-D [*Šimůnek et al.*, 2009] (see auxiliary material). A significant advantage of this model is that it side steps the need to consider the transient flow dynamics of infiltration and redistribution. Each infiltration event leads to an instantaneous displacement of the point load (or its centroid), using the assumption that a field capacity water content (representing no further advective solute transport) can be used to predict the final postredistribution profile of water and solute. Thus, we do not have to deal with the complexities of transient flow for each event or the associated computational difficulties. The results suggested that

Table 4. Dimensionless Numbers Characterizing the Hydrologic and Solute Transport Behavior of Four Soil-Climate Combinations and Four Common Pesticides[a]

	ϕ	γ	Ω	Atrazine				Bromacil				Ethylene Dibromide				Oxamyl			
				κ/Ω	$RF\gamma$	$k\mu_T$	$k\mu_{T0}$	κ/Ω	$RF\gamma$	$k\mu_T$	$k\mu_{T0}$	κ/Ω	$RF\gamma$	$k\mu_T$	$k\mu_{T0}$	κ/Ω	$RF\gamma$	$k\mu_T$	$k\mu_{T0}$
Coarse humid	0.65	5.9	0.46	0.078	63	3.4	2.3	0.014	35	0.33	0.23	0.001	25	0.024	0.016	0.83	13	7.3	5.0
Coarse arid	2.5	2.1	0.26	0.88	23	10	5.3	0.16	13	1.0	0.53	0.015	9.2	0.073	0.037	9.4	4.7	22	11
Fine humid	0.65	24	0.39	0.092	360	21	13	0.017	180	1.9	1.2	0.002	120	0.12	0.078	0.98	46	28	18
Fine arid	2.5	8.6	0.029	7.9	13	180	30	1.4	65	16	2.7	0.14	45	1.1	0.18	84	17	240	41

[a]The first two numbers, ϕ and γ, represent the aridity index and the storage capacity of the soil relative to the average storm, respectively. Ω is the recharge ratio (mean rate of recharge versus infiltration), and κ/Ω determines whether the transport through the soil is dominated by the mean travel time or large, rare events. $RF\gamma$ is a measure of the number of storms required to transport the solute through the soil. The products $k\mu_T$ and $k\mu_{T0}$ are the Damköhler numbers for the cases with and without evapotranspiration. Several of these dimensionless numbers are also given in Figure 2.

the simple model did a reasonable job of predicting the total loads and their temporal dynamics. By combining this model with the stochastic soil water models developed in recent years, semianalytic expressions for the pdf of solute travel time and delivery ratio were derived. These expressions were found to predict the results of the piston displacement model very well.

[81] The resulting expressions were used to obtain the following insights.

[82] 1. The results suggest that the mean and variance of the travel time are increased by the action of evapotranspiration. In particular, the mean travel time was found to be determined by the geometric mean of the time-averaged infiltration at the top of the soil profile and recharge rates at the base. This effect could be expressed as a function of the recharge ratio Ω.

[83] 2. While the mean travel time increased with soil depth in all climates, the coefficient of variation in travel time decreased with increasing soil thickness in wet climates and increased with soil thickness in dry climates. In wet climates each event transports the solutes slightly deeper in the profile, and so the total travel time averages over the variability of many events. In contrast, in dry climates, solutes build up in the profile, where they remain inaccessible to transport until a large event flushes the profile.

[84] 3. The distribution of the delivery ratio was found to be dependent on Ω and a second dimensionless number κ. For small values of κ the delivery ratio is mean time dependent: the mean delivery ratio approaches that predicted by the mean travel time. However, for large values of κ the delivery ratio is fast time dependent and is affected by the probability of a single large event carrying the solute all the way through the system. For such fast time–dependent solutes these relatively rare events may be the primary mechanism for transport to groundwater systems.

[85] 4. The results were used to classify the controls on the delivery of four common pesticides applied to four soil-climate combinations. Under the humid climate, the slower degrading compounds atrazine, bromacil, and ethylene dibromide were found to be mean time dependent. Under dry climates their behavior was mixed or even fast time dependent depending on the soil type. Under dry climates the fast degrading oxamyl was fast time dependent, but under a humid climate it was mixed.

[86] The results of this work could be used to better understand the risk of pesticide leaching and the controls on it, though the methods are not limited to pesticides. It can also be used to assess the risks posed by climate change, which may alter the frequency of storm events, their magnitude, or the evapotranspiration or all of these. An increase in total storm depth with little increase in total precipitation would correspond to a decrease in γ. The results here suggest that this could lead to an increase in the delivery ratio in a dry area but may have less significance in a wet area.

[87] Our focus in this paper is systems without significant preferential flow and in which infiltration produces fairly uniform wetting fronts. However, the approach can be potentially modified to consider such effects.

[88] In this work the effect of dispersion has been neglected in favor of analyzing the effect of the temporal variability imposed by the climate and vegetation water

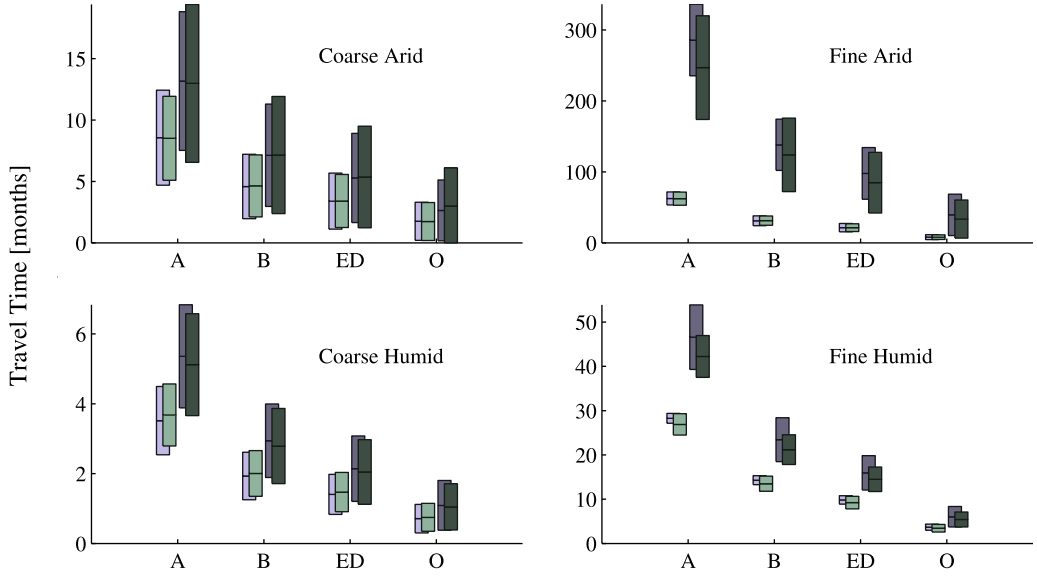

Figure 12. Each darker pair of bars gives the mean (center of the bar) and standard deviation (length of the bar) of the travel time (in days) predicted by the numerical model (back bar in each pair) and its analytical approximation (front bar; equation (33)) for various pesticides under the four example scenarios. Lighter bars show the mean and standard deviation when the effects of evapotranspiration are neglected (back bar is numerical result, and front bar is analytical approximation).

uptake. We see several ways in which future work may address the dispersion issue within this framework. As *Rao et al.* [1985a] suggest, if the spreading of the plume is proportional to transport distance, the concentration profile of the soil can be easily calculated, as can the flux through the control plane at the base of the zone being modeled. Alternatively, a Lagrangian approach akin to particle tracking could be adopted in which a population of point loads is introduced into the profile. Dispersion would be represented by introducing a random component to their jump sizes in each transport event. Furthermore, we have neglected the effects of preferential flow. Future work could seek to combine the approach used here with that of *McGrath et al.* [2008b] to develop a more complete approach.

[89] We have also assumed that the vertical profile of soil chemical properties is constant. In many soils the

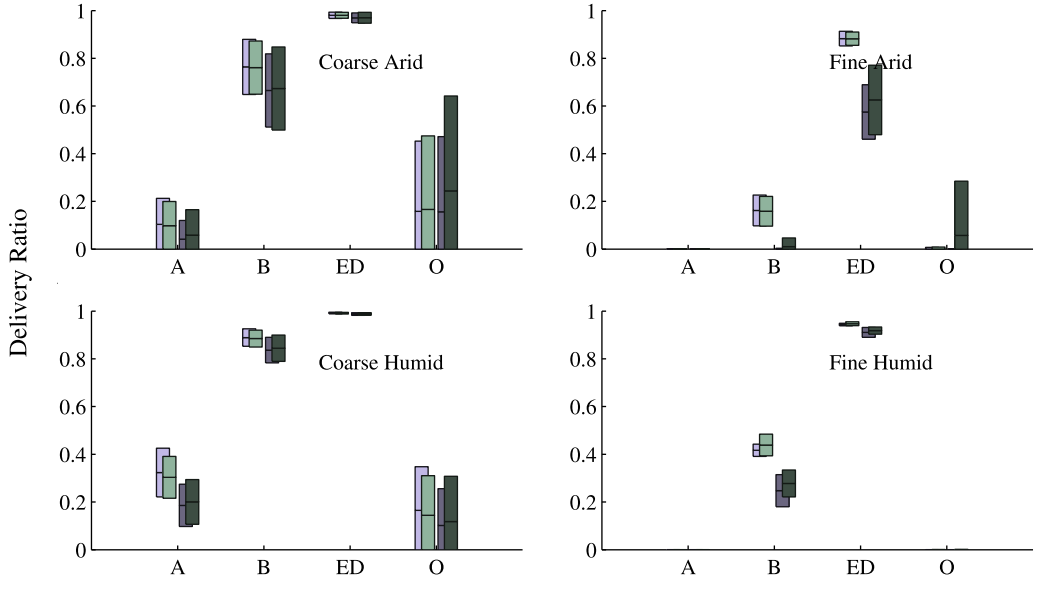

Figure 13. Darker pair of bars shows mean (center of the bar) and standard deviation (length of the bar) of the delivery ratio predicted by the numerical model (lower bar in each pair) and its analytical approximation (upper bar; equation (35)) for the example scenarios. Lighter bars show the mean and standard deviation when the effects of evapotranspiration are neglected (lower bar is numerical result, and upper bar is analytical approximation).

reactivity and chemical sorption processes vary with depth because of variations in organic matter content, availability of electron acceptors, and mineralogy [*Issa and Wood*, 1999]. These profiles have the potential to interact with the vertical profile of transport rates investigated here in interesting ways. If the sorption and reaction rates at depth (where transport is slowed by the storage deficit) are lower than at the surface (where transport is more rapid), the deceleration of a plume due to evapotranspiration may be partially compensated by the increased transport capacity and greater retention. These intriguing possibilities are left for future work.

[90] By introducing the effect of evapotranspiration this work has built on the previous efforts of *Jury and Gruber* [1989], but there is considerable room to further explore this issue. The assumptions regarding water uptake produce a particular pattern of root water uptake within the profile. If bare soil evaporation or a different root profile were incorporated, the storage deficit in the profile would evolve in a different way, producing a different vertical profile in the distribution of waiting times as a function of depth. We might expect that bare soil evaporation would increase the storage deficit in the upper few centimeters of the soil. However, we have also assumed that the vegetation extracts water from the whole profile, including the surface. Root distributions generally peak below the soil surface [*Schenk and Jackson*, 2002]. If this profile were included, the extraction at the surface would decrease. Therefore, it is unclear whether the combined effects of relaxing these assumptions would increase or decrease the storage deficit in the surface soils. Further work may determine whether these effects are significant.

[91] The work presented here offers a framework for doing comparative hydrology; that is, it can be used to tease apart the fundamental differences between watersheds that lead to their differing functional behavior. Comparative hydrology is also the appropriate basis for testing the model. The results from an individual lysimeter or soil column are not sufficient, as they would constitute a sample size of $n = 1$ with respect to testing the main predictions described here. Future work building on these results will be concerned with testing whether the results are able to explain patterns of variation in travel time across different climates and soils by compiling data from a range of studies from the laboratory to watershed-scale tracer studies.

[92] **Acknowledgments.** Work on this paper commenced during the Summer Institute organized at the University of British Columbia (UBC) during June–July 2009 as part of the NSF-funded Hydrologic Synthesis project, "Water Cycle Dynamics in a Changing Environment: Advancing Hydrologic Science through Synthesis" (NSF grant EAR 06-36043, M. Sivapalan, PI). The work was completed with support from NSF grant EAR 09-11205, "Biotic alteration of soil hydrologic properties and feedback with vegetation dynamics in water limited ecosystems" (M. Sivapalan, PI). Support from NSF grant ATM 06-28687 is also gratefully acknowledged. Thanks also go to Al Valocchi and Stefano Zanardo for their fruitful discussions of these ideas. Andrew Guswa, Erwin Zehe and an anonymous reviewer provided useful suggestions that improved the quality of the manuscript.

References

Abramowitz, M., and I. A. Stegun (1972), *Handbook of Mathematical Functions*, Dover, New York.

Arias-este, M., E. Lopez-Periago, E. Martinez-Carballo, J. Simal-Gandara, J.-C. Mejuto, and L. Garcia-Rio (2008), The mobility and degradation of pesticides in soils and the pollution of groundwater resources, *Agric. Ecosyst. Environ.*, *123*, 247–260, doi:10.1016/j.agee.2007.07.011.

Basu, N. B., S. E. E. Thompson, and S. C. Rao (2011), Hydrologic and biogeochemical functioning of intensively managed catchments: A synthesis of top-down analyses, *Water Resour. Res.*, doi:10.1029/2011WR010800, in press.

Bengough, A. G., M. F. Bransby, J. Hans, S. J. McKenna, T. J. Roberts, and T. A. Valentine (2006), Root responses to soil physical conditions; growth dynamics from field to cell, *J. Exp. Bot.*, *57*(2), 437–447, doi:10.1093/jxb/erj003.

Botter, G., A. Porporato, I. Rodriguez-Iturbe, and A. Rinaldo (2007), Basin-scale soil moisture dynamics and the probabilistic characterization of carrier hydrologic flows: Slow, leaching-prone components of the hydrologic response, *Water Resour. Res.*, *43*, W02417, doi:10.1029/2006WR005043.

Destouni, G. (1991), Applicability of the steady state flow assumption for solute advection in field soils, *Water Resour. Res.*, *27*(8), 2129–2140, doi:10.1029/91WR01115.

Domenico, P., and F. Schwartz (1990), *Physical and Chemical Hydrogeology*, pp. 296–302, John Wiley, New York.

Eagleson, P. S. (1978), Climate, soil, and vegetation: 6. Dynamics of the annual water balance, *Water Resour. Res.*, *14*(5), 749–764, doi:10.1029/WR014i005p00749.

Feddes, R. A., P. J. Kowalik, and H. Zaradny (1978), *Simulation of Field Water Use and Crop Yield*, John Wiley, New York.

Fiori, A., and D. Russo (2008), Travel time distribution in a hillslope: Insight from numerical simulations, *Water Resour. Res.*, *44*, W12426, doi:10.1029/2008WR007135.

Flury, M. (1996), Experimental evidence of transport of pesticides through field soils—A review, *J. Environ. Qual.*, *25*(1), 25–45, doi:10.2134/jeq1996.00472425002500010005x.

Foussereau, X., W. D. Graham, G. Akpoji, G. Destouni, and P. S. C. Rao (2001), Solute transport through a heterogeneous coupled vadose-saturated zone system with temporally random rainfall, *Water Resour. Res.*, *37*(6), 1577–1588, doi:10.1029/2000WR900389.

Green, W. G., and G. Ampt (1911), Studies of soil physics, I: The flow of air and water through soils, *J. Agric. Sci.*, *4*, 1–24.

Gustafson, D. I. (1989), Groundwater ubiquity score: A simple method for assessing pesticide leachability, *Environ. Toxicol. Chem.*, *8*(4), 339–357, doi:10.1002/etc.5620080411.

Guswa, A. J., M. A. Celia, and I. Rodriguez-Iturbe (2004), Effect of vertical resolution on predictions of transpiration in water-limited ecosystems, *Adv. Water Resour.*, *27*(5), 467–480.

Hawk, K. L., and P. S. Eagleson (1992), Climatology of station storm rainfall in the continental United States: Parameters of the Bartlett-Lewis and Poisson rectangular pulses models, technical report 336, Ralph M. Parsons Lab., Dep. of Civ. and Environ. Eng., Mass. Inst. of Technol., Cambridge.

Hornsby, A. G., R. D. Wauchope, and A. E. Herner (1996), *Pesticide Properties in the Environment*, Springer, New York.

Issa, S., and M. Wood (1999), Degradation of atrazine and isoproturon in the unsaturated zone: A study from southern England, *Pesticide Sci.*, *55*(5), 539–545, doi:10.1002/(SICI)1096-9063(199905)55:5<539::AID-PS970>3.0.CO;2-8.

Jury, W. A., and J. Gruber (1989), A stochastic analysis of the influence of soil and climatic variability on the estimate of pesticide groundwater pollution potential, *Water Resour. Res.*, *25*(12), 2465–2474, doi:10.1029/WR025i012p02465.

Jury, W. A., L. H. Stolzy, and P. Shouse (1982), A field test of the transfer function model for predicting solute transport, *Water Resour. Res.*, *18*(2), 369–375, doi:10.1029/WR018i002p00369.

Laio, F. (2006), A vertically extended stochastic model of soil moisture in the root zone, *Water Resour. Res.*, *42*, W02406, doi:10.1029/2005WR004502.

Laio, F., A. Porporato, L. Ridolfi, and I. Rodriguez-Iturbe (2001), Mean first passage times of processes driven by white shot noise, *Phys. Rev. E*, *63*(3), 036105.

Laio, F., P. D'Odorico, and L. Ridolfi (2006), An analytical model to relate the vertical root distribution to climate and soil properties, *Geophys. Res. Lett.*, *33*, L18401, doi:10.1029/2006GL027331.

McGrath, G. S. (2007), An exploration of rainfall controls on pesticide transport via fast flow pathways, Ph.D. thesis, 156 pp., Sch. of Earth and Geogr. Sci., Univ. of West. Aust., Crawley, West. Aust., Australia.

McGrath, G. S., C. Hinz, and M. Sivapalan (2007), Temporal dynamics of hydrological threshold events, *Hydrol. Earth Syst. Sci. 11*(2), 923–938, doi:10.5194/hess-11-923-2007.

McGrath, G. S., C. Hinz, and M. Sivapalan (2008a), Modeling the effect of rainfall intermittency on the variability of solute persistence at the soil surface, *Water Resour. Res.*, *44*, W09432, doi:10.1029/2007WR006652.

McGrath, G. S., C. Hinz, and M. Sivapalan (2008b), Modelling the impact of within-storm variability of rainfall on the loading of solutes to preferential flow pathways, *Eur. J. Soil Sci.*, *59*, 24–33.

McGrath, G., C. Hinz, and M. Sivapalan (2010a), Assessing the impact of regional rainfall variability on rapid pesticide leaching potential, *J. Contam. Hydrol.*, *113*(1–4), 56–65, doi:10.1016/j.jconhyd.2009.12.007.

McGrath, G. S., C. Hinz, M. Sivapalan, J. Dressel, T. Pütz, and H. Vereecken (2010b), Identifying a rainfall event threshold triggering herbicide leaching by preferential flow, *Water Resour. Res.*, *46*, W02513, doi:10.1029/2008WR007506.

Milly, P. (1985), Stability of the Green-Ampt profile in a delta function soil, *Water Resour. Res.*, *21*(3), 399–402, doi:10.1029/WR021i003p00399.

Milly, P. C. D. (1993), An analytic solution of the stochastic storage problem applicable to soil water, *Water Resour. Res.*, *29*(11), 3755–3758, doi:10.1029/93WR01934.

Ocampo, C., C. Oldham, and M. Sivapalan (2006), Nitrate attenuation in agricultural catchments: Shifting balances between transport and reaction, *Water Resour. Res.*, *42*, W01408, doi:10.1029/2004WR003773.

Porporato, A., F. Laio, L. Ridolfi, and I. Rodriguez-Iturbe (2001), Plants in water-controlled ecosystems: Active role in hydrologic processes and response to water stress, III. Vegetation water stress, *Adv. Water Resour.*, *24*(7), 725–744, doi:10.1016/S0309-1708(01)00006-9.

Porporato, A., E. Daly, and I. Rodriguez-Iturbe (2004), Soil water balance and ecosystem response to climate change, *Am. Nat.*, *164*(5), 625–632, doi:10.1086/424970.

Raats, P. A. C. (1981), Residence times of water and solutes within and below the root zone, *Agric. Water Manage.*, *4*(1–3), 63–82, doi:10.1016/0378-3774(81)90044-5.

Rao, P. S. C., and J. M. Davidson (1980), Estimation of pesticide retention and transformation parameters required in nonpoint source pollution models, in *Environmental Impact of Nonpoint Source Pollution*, edited by M. Overcash and J. Davidson, pp. 23–67, Ann Arbor Sci., Ann Arbor, Mich.

Rao, P. S. C., R. E. Jessup, and J. M. Davidson (1985a), Mass flow and dispersion, in *Environmental Chemistry of Herbicides*, vol. 1, edited by R. Grover, chap. 4, pp. 21–45, CRC Press, Boca Raton, Fla.

Rao, P. S. C., G. Hornsby, and R. E. Jessup (1985b), Indices for ranking the potential for pesticide contamination of groundwater, *Proc. Soil Crop Sci. Soc. Fla.*, *44*, 1–8.

Rodriguez-Iturbe, I., A. Porporato, L. Rldolfi, V. Isham, and D. R. Cox (1999), Probabilistic modelling of water balance at a point: The role of climate, soil and vegetation, *Proc. R. Soc. London, Ser. A*, *455*(1990), 3789–3805.

Russo, D., and A. Fiori (2008), Equivalent vadose zone steady state flow: An assessment of its capability to predict transport in a realistic combined vadose zone-groundwater flow system, *Water Resour. Res.*, *44*(9), 1–19, W09436, doi:10.1029/2007WR006170.

Russo, D., W. A. Jury, and G. L. Butters (1989a), Numerical analysis of solute transport during transient irrigation: 2. The effect of immobile water, *Water Resour. Res.*, *25*(10), 2119–2127, doi:10.1029/WR025i010p02119.

Russo, D., W. A. Jury, and G. L. Butters (1989b), Numerical analysis of solute transport during transient irrigation: 1. The effect of hysteresis and profile heterogeneity, *Water Resour. Res.*, *25*(10), 2109–2118, doi:10.1029/WR025i010p02109.

Saxton, K. E., and W. J. Rawls (2006), Soil water characteristic estimates by texture and organic matter for hydrologic solutions, *Soil Sci. Soc. Am. J.*, *70*(5), 1569–1578, doi:10.2136/sssaj2005.0117.

Schenk, H. J. (2008), The shallowest possible water extraction profile: A null model for global root distributions, *Vadose Zone J.*, *7*(3), 1119–1124, doi:10.2136/vzj2007.0119.

Schenk, H. J., and R. Jackson (2002), The global biogeography of roots, *Ecol. Monogr.*, *72*(3), 311–328.

Šimůnek, J., M. Šejna, H. Saito, M. Sakai, and M. T. van Genuchten. (2009), The HYDRUS-1D software package for simulating the movement of water, heat, and multiple solutes in variably saturated media, technical report, Dep. of Environ. Sci., Univ. of Calif., Riverside.

Struthers, I., C. Hinz, and M. Sivapalan (2006), A multiple wetting front gravitational infiltration and redistribution model for water balance applications, *Water Resour. Res.*, *42*, W06406, doi:10.1029/2005WR004645.

Struthers, I., C. Hinz, and M. Sivapalan (2007), Conceptual examination of climate-soil controls upon rainfall partitioning in an open-fractured soil, II: Response to a population of storms, *Adv. Water Resour.*, *30*(3), 518–527, doi:10.1016/j.advwatres.2006.04.005.

Troch, P. A., G. F. Martinez, V. R. N. Pauwels, M. Durcik, M. Sivapalan, C. Harman, P. D. Brooks, H. Gupta, and T. Huxman (2009), Climate and vegetation water use efficiency at catchment scales, *Hydrol. Processes*, *23*(16), 2409–2414, doi:10.1002/hyp.7358.

van Der Werf, H. M. G. (1996), Assessing the impact of pesticides on the environment, *Agric. Ecosyst. Environ.*, *60*, 81–96, doi:10.1016/S0167-8809(96)01096-1.

Wang, P., P. Quinlan, and D. M. Tartakovsky (2009), Effects of spatio-temporal variability of precipitation on contaminant migration in the vadose zone, *Geophys. Res. Lett.*, *36*, L12404, doi:10.1029/2009GL038347.

Wierenga, P. J. (1977), Solute distribution profiles computed with steady-state and transient water movement models, *Soil Sci. Soc. Am. J.*, *41*(6), 1050–1055, doi:10.2136/sssaj1977.03615995004100060006x.

N. B. Basu, Department of Civil and Environmental Engineering, University of Iowa, Iowa City, IA 52242, USA.

C. J. Harman, P. Kumar, and M. Sivapalan, Department of Civil and Environmental Engineering, University of Illinois at Urbana-Champaign, Hydrosystems Building, MC 250, 205 N. Mathews Ave., Urbana, IL 61801, USA. (charman2@uiuc.edu)

G. S. McGrath, School of Earth and Environment, University of Western Australia, Crawley, WA 6009, Australia.

P. S. C. Rao, School of Civil Engineering, Purdue University, West Lafayette, IN 47907, USA.